PERFORMANCE ENHANCEMENT OF SILVER-NANOPARTICLE/TITANIA ($Ag\text{-}NP/TiO_2$) USING CHLOROPHYLL AS DYE SENSITIZER

A RESEARCH THESIS SUBMITTED IN PARTIAL FULFILMENT

OF THE REQUIREMENTS FOR THE DEGREE OF

MASTER OF SCIENCE IN CHEMISTRY

OF

THE UNIVERSITY OF NAMIBIA

BY

LOINI MAGANO KALIPI

(201136503)

April 2019

Main supervisor: Dr. L. S. Daniel (Dep. of Chemistry and Biochemistry Department)

Co-supervisor: Dr. V. Uahengo (Dep. of Chemistry and Biochemistry Department)

ABSTRACT

Titanium dioxide or titania (TiO_2) being one of the most promising semiconductors for many photoelectrochemical applications, its utilization remains typically confined to ultraviolet (UV) light absorption because of its wide band gap (3.2 eV for anatase and 3.0 eV for rutile), where by UV only accounts for 4-6% of the solar radiation. There is a need to shift the absorption threshold of the UV-region response of TiO_2 into the visible region (accounts for ~45% of the total energy of the solar radiation), which can be achieved by doping TiO_2 with dye sensitizers, non-metals, transition metals or through surface plasmon resonance (SPR) using noble metals. To study the absorption spectra of metallic silver nanoparticle/titania/Chlorophyll (Ag-NP/TiO_2/Chlorophyll) thin films, sandwich arrangement thin films were fabricated on a quartz glass substrate at 550°C using a spin coater. Respective precursor solutions for Ag-nanoparticles and titania were prepared from Ag salt and a titanium complex using molecular precursor method. The Chlorophyll dye was extracted from the *Colophospermum mopane* leaves (Mopane tree leaves) and *Hyphaene petersiana* leaves (Makalani tree leaves) using methanol as a solvent extract. The Ag-nanoparticle/TiO_2 (Ag-NP/TiO_2) thin films were then immersed in the Chlorophyll dye for 48 hours, to produce Ag-NP/TiO_2/Chlorophyll dye composites thin films. A Fourier-transform infrared (FTIR) spectrum was used to confirm whether the dye extract was chlorophyll. The absorption properties of the thin films were studied using Ultraviolet-visible (UV-VIS) Spectrophotometer. The absorption of the entire visible region for the Ag-NP/TiO_2 composite thin films was stronger than that for the undoped TiO_2 thin film. This is due to the generation of the absorption peak attributed to the surface plasmon resonance (SPR) of metallic silver

nanoparticles in the TiO_2 matrix, which exhibited a broad band, improving the absorption throughout the entire visible region. Undoped TiO_2 thin film showed no absorbance in the visible region. The pure Chlorophyll thin films showed two stronger absorption peaks at the wavelength of 415 nm to 665 nm respectively. Apart from a surface plasmon resonance (SPR) peak around 410 nm, additional wide-range absorption spread in the vis-region at wavelengths greater than 410 nm was observed for Ag-NP/TiO_2/Chlorophyll dye thin films. The wide-range absorption is due to the coupling between the dye and plasmon resonance properties of the Ag-nanoparticles. The band gap of the fabricated thin films is in the range of 1.4 and 3.50 eV, with 75%Ag-NP/TiO_2/Chlorophyll dye thin film with the lowest band gap of 1.4 eV and the highest band gap of 3.50 eV obtained from an undoped TiO_2 thin film. The reduction in bandgap is due to metal – ligand charge transfer (MLCT) transition, through which the photoelectric charge of low-lying empty orbitals such as CO or CN^- possessed by chlorophyll injected into the TiO_2 band gap. The wide-range absorption observed is therefore clarified by SPR and bandgap narrowing. On the basis of absorption spectra analysis, a plasmonic-band gap narrowing mechanism was proposed.

TABLE OF CONTENT

LIST OF TABLES

LIST OF FIGURES

LIST OF ABBREVIATIONS

TiO_2	Titanium dioxide/Titania
UV-VIS	Ultraviolet-visible
eV	Band gap energy
MLCT	Metal – ligand charge transfer
Ag-NPs	Silver Nanoparticles
SPR	Surface Plasmon Resonance
LSPR	Localized Surface Plasmon Resonance
Ag-NP/TiO_2	Silver Nanoparticles/Titania composite
DSSCs	Dye Sensitizer Solar Cells
ZnO	Zinc Oxide
SnO_2	Tin Dioxide
CuO	Copper Oxide
CoO	Cobalt Oxide
TEM	Transmission Electron Microscopy
XRD	X-ray diffraction
MPM	Molecular precursor method
$Ti(OiPr)_4$	Titanium tetraisopropoxide
EDTA	ethylenediamine-N,N,N',N'- tetraacetic acid

ρ	Resistivity
λ	Wavelength
K	Kelvin
V	Voltage
V_{OC}	Open circuit voltage
I_{SC}	Short circuit voltage
FF	Fill factor
nm	nanometer
HOMO	highest occupied molecular orbital
LUMO	lowest unoccupied molecular orbital
NIR	near-infrared
A	absorbance
T	transmittance
ε	molar absorptivity or the molar extinction coefficient
ΔE	energy of radiation
FTIR	Fourier transform infrared
IR	Infrared
Eg	Band gap

PVD	physical vapor deposition
CVD	chemical vapor deposition
ALE	atomic layer epitaxy

ACKNOWLEDGEMENTS

I would like to thank the Almighty God for the guidance and protection he had given me, and for helping me to successfully complete my study. I acknowledge and thank Dr. Daniel Likius and Dr Veikko Uahengo (both from UNAM's Faculty of Science, Chemistry and Biochemistry Department) for the academic supervision they have given me, I really appreciate their help.

I would like to express my sincere appreciation to the Ministry of Education and National Commission on Research Science and Technology, through the NCRST under the call to strengthen research capacity at universities and research institutions (April 2017 to March 2020) from research grant awarded to the research project titled "Renewable Energy Initiative Project" for funding my studies. I would also love to acknowledge the University of Namibia, Department of Chemistry and Biochemistry; and the Center for Postgraduate Studies for providing my research with the necessary equipment, reagents and laboratory I needed during my studies.

Lastly I would like to sincerely thank Prof Edet Archibong, Theopolina Thomas, Johannes Naihmwaka, Ester Kalipi, Johanna Kalipi, Titus Kalipi, Matheus Shilume, Paulina Endjala, family and friends for their effortless support, encouragement and for always believing in me.

DEDICATION

To my parents, Johanna Kalipi and Titus Kalipi for their effortless support.

DECLARATIONS

I, Loini Magano Kalipi, hereby declare that this study is my own work and is a true reflection of my research, and that this work, or any part thereof has not been submitted for a degree at any other institution.

…… ..……. ……..……..……

Name of Student Signature Date

CHAPTER 1: INTRODUCTION

1.1 Background of the study

TiO_2 is a white inorganic solid substance and one of the most promising semiconductors for many photoelectrochemical applications, due to its low cost, chemical stability and non-toxicity [1]. TiO_2 can be used in products such as paints and coatings, including glazes and enamels, plastics, photocatalyst, dye sensitized solar cells, integrated circuits, paper, inks foods, pharmaceuticals and cosmetics [1, 2, 3]. TiO_2 have three main polymorphs, anatase (tetragonal), rutile (tetragonal) and brookite (orthorhombic); and the primary and the most stable of the all is rutile ore [4, 3] as shown in figure 1. Rutile has high temperature phase (600–1855°C), whereas anatase and brookite are metastable and are readily transformed to rutile when heated [5].

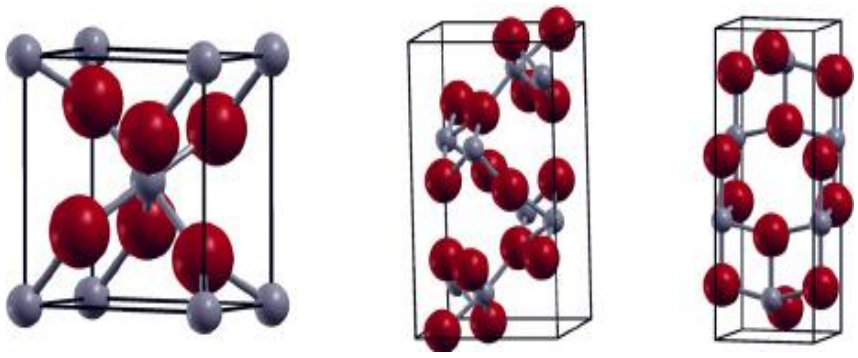

(a) (b) (c)

Figure 1 Crystalline structures of titanium dioxide (a) rutile, (b) brookite, (c) anatase [3, 6].

TiO_2 is an n-type semiconductor that has a band gap in the range of 3.0 - 3.2 eV (3.2 eV for anatase, 3.0 eV for rutile, and ~3.2 eV for brookite) [1, 4, 7,]. Due to this wide band gap, the utilization of TiO_2 remains typically confined to ultraviolet (UV) light [1], which accounts for only 4-6% of solar radiation as illustrated in figure 2, limiting the efficient utilization of solar energy by TiO_2. It is noted that visible light with spectral wavelength between 400 and 700 nm accounts for about 40% of the total energy of the solar radiation.

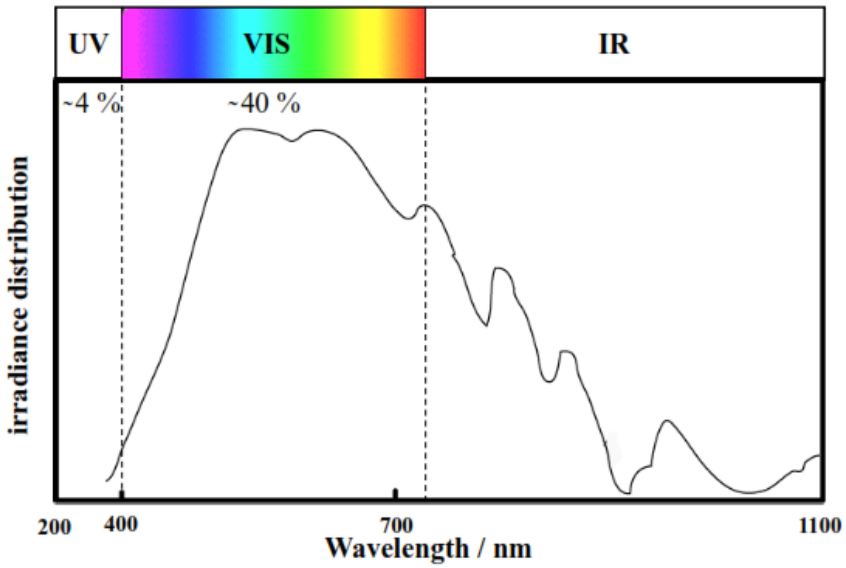

Figure 2 The standard solar spectra irradiance (AM1.5 global = one sun) [4].

For this reason, many attempts have been undertaken in recent decades to shift the threshold of the photo-response of TiO_2 into the visible region, which would enhance its potential for chemical solar energy conversion [8]. Shifting the threshold of the photo-response of TiO_2 into the visible region can be achieved by doping TiO_2 with a foreign substance, such as sensitizers, noble metals, transition metal etc [4, 9].

There are different types of dye sensitizer, natural, inorganic and organic dyes and they all imitate the way in which plant harness solar energy [10]. The considerable advantage of these dyes lies in the metal – ligand charge transfer (MLCT) transition, through which the photoelectric charge is injected into the TiO_2 [11,10]. MLCT happens when the metal is in a low oxidation state (meaning electron rich) and the ligand possesses low – lying empty orbitals (e.g., CO or CN^-) then the transition will occur [11]. Due to high costs, presence of heavy metals, and complex synthesis processes of the inorganic and organic dyes, natural dyes are getting more attention because they are cutting down high cost of metal complex sensitizers; they are replacing expensive chemical synthesis process through simple extraction process [12, 13]. Natural dyes are abundant, easily extractable, they are safe – they cause no environment threat, they are nontoxic and completely biodegradable [14]. There are different types of natural dye sensitizers; anthocyanin, carotenoid, flavonoid and chlorophyll pigments to mention a few and they are extracted either from flowers petals, roots, leaves, fruits, and plants [12, 14, 15, 16]. However, stability problem results in less efficiency.

With noble metals, such as gold and silver nanoparticles possess a unique property called "Surface Plasmon Resonance" which is the interaction of metallic nanoparticle with visible light to create a collective oscillation of the conduction electron [17]. These metallic nanoparticles are used to dope TiO_2 to improve the photo-response, which can be studied using thin films. In this research, the TiO_2 was doped with the synthesized noble metal (silver) and extracted dye sensitizer (chlorophyll).

1.2 Statement of the problem

TiO_2 absorbs photons in the UV region, which only accounts for 4-6% of the solar radiation. There is a need to shift the threshold of the photo-response of TiO_2 into the visible region, which can be achieved by doping TiO_2 with foreign substances such as noble metals, dye sensitizers, non-metals and transition metals.

1.3 Objectives

The main purpose of this study is to elucidate the mechanism of vis-light-excited electron transfer occurring in the Ag-NP/TiO_2/Chlorophyll composite thin film system by examining the absorption spectra. In order to achieve this, the following objectives were carried out.

The objectives of the study were to:

(a) Extract Chlorophyll dye from the leaves

(b) Fabricate Ag-NP/TiO_2 and Ag-NP/TiO_2/Chlorophyll dye sensitizers composites thin films.

(c) Characterize the absorption properties of the fabricated thin films.

1.4 Significance of the study

This study provides information that Chlorophyll as dye sensitizers can improve the performance in Ag-NP/TiO_2 composite thin films, hence shifting the threshold of photo-response of TiO_2 into the visible region. This can contribute to the improvement of the

efficiency of the dye sensitizer solar cells (DSSCs), as it increases the absorbance of the Ag-NP/TiO_2 in the visible and near infrared region.

1.5 Limitation of the study

The distribution and structural properties of Ag-NP on the thin films was not investigated, because equipment used to investigate those properties; Transmission Electron Microscopy (TEM) and the X-ray Diffraction (XRD) are not available at UNAM.

1.6 Delimitation of the study

The research focus was on the optical properties of the composite thin films and adsorbent of the dye sensitizer on the Ag-NP/TiO_2 thin films and not on photoelectrochemical cells (DSSCs).

CHAPTER 2: LITERATURE REVIEW

2.1 Overview

There is a need to move towards a low carbon economy and this has led to unprecedented interest in renewables energy resources [11]. Other renewables energy resources are wind, hydro, biomass and geothermal, but solar energy is the fundamental renewable resources accessible today as it provides energy for all living creatures on earth [12]. Solar energy is readily available, non-toxic, no noise pollution, no greenhouse gas emissions. Richhariya and his group defined solar energy as a renewable electrical energy that is obtained directly from the sun as absorbed photons [12], in order to convert the solar energy into direct current electricity, photovoltaics are used. Photovoltaics are defined as method for generating electric power by using solar cells to convert energy from the sun into a flow of electrons [18]. The first generation of solar cell consists of monocrystalline silicon solar cell, which is made up of silicon wafers; the second generation of solar cell is the thin film solar cell-basically these are the amorphous silicon solar cell; and the third generation is the nanocrystal and polymer based solar cells, the generation of dye sensitized solar cells [19].

Solar converters such as such as solar panel should be able to absorb light in the visible light region and they are made up of semiconductors materials such as TiO_2, ZnO, SnO_2, CuO, CoO etc. The semiconductors have excellent properties such as; good stability; less reactivity; low toxicity, availability and capability of moving the photo-generated electrons [1]. TiO_2 being one the most promising abundantly semiconductor, it is regarded as an efficient photocatalyst, where its application is extended to self-cleaning

building materials and environment preservation technologies [20]. The other semiconductors are unstable due to inappropriate dissolution (especially ZnO), leading to catalyst inactivation over time [21]; or less photocatalytically active than TiO_2 [22].

TiO_2 semiconductor is currently the most actively and widely investigated semiconductors for applications that can effectively address environmental pollution [23] and at a smaller scale (micro), the white crystal of TiO_2 they become increasingly colorless as the crystals shrink in size, and their colloids become invisible to the human eye below about 15 nm [24]. Due to the TiO_2 restriction in the UV region, doping of a foreign element, such as Ag, Cr, V, Fe, Mn, Co, and Ni, into Ti sites; and that of anions, such as N, S, and C, into O sites have been tested [2, 22, 25] to enhance its absorption and photocatalytically potential.

2.2 Doping TiO_2 systems

Researchers derived techniques on how to introduce foreign elements into the parent photocatalyst without giving rise to new crystallographic forms, phases or structures and the purpose is to improve the net separation of photogenerated charges, hence improving the light harvesting of TiO_2 from ultraviolet region to the visible region (accounts for ~45% of total energy radiation) [25].

2.2.1 Doping TiO_2 systems with non-metals

The study done by Asahi and his group, reported that nitride ion, causes TiO_2 to respond to Vis light at the oxygen sites of TiO_2, due to the presence of nitrogen that narrows the

band gap of TiO_2 making it capable of performing visible light driven photocatalysis [4]. Since these discoveries, nonmetals has been extremely investigated and up to date it is well known that non-metals such a nitrogen, carbon and sulphur impurity in TiO_2 matrix shift the energy levels above the parent TiO_2 valence enabling the thin film to be responsive to Vis light [4].

2.2.2 Doping TiO_2 systems with transition metal

Various transition metals and transition metal ions such as Co, V^{5+}, Cr^{3+}, and Cu^{2+} into the lattice of Ti^{4+} in anatase thin films are investigated, it was found that the photoreactivities of chemically modified TiO_2 thin films is reduced under UV irradiation and the thin films modified with transition-metal ions can now response to Vis-light irradiation [4]. Hiroshi et al [20] reported that attaching Cu(II) on the surfaces of TiO_2, leads to the production of visible-light-sensitive photocatalysts and it is triggered by the photo-induced interfacial charge transfer from the valence band of oxides to Cu(II) ions. The resistivity of TiO_2 have a tendency to reduce when doped, the research done by Karabay and his group, Karabay et al [2] found that the resistivity of the samples of TiO_2 ($\rho \cong 4.5 \times 10^9 \Omega cm$) is reduced to $\rho \cong 7.1 \times 10^8 \Omega cm$ when doped with Cobalt. Although doping the semiconductor with transitions metals offers good results, it may also act as recombination site for the photo-induced charge carriers, which lowers down quantum efficiency; can also cause thermal instability to the TiO_2 nanomaterial; and does not remarkably enhanced the photocatalytic activity, because metals introduced are not incorporated into the TiO_2 framework [4, 20].

2.2.3 Doping TiO_2 systems with noble metals

Noble metals are defined as metals (e.g. gold, silver, or platinum) that resist chemical action, do not corrode, and are not easily attacked by acids. Incorporation of nanoparticles into semiconductors has been extensively studied for many years [26, 27, 28], where TiO_2 have been the focus, this is because its resistivity (10^{12} Ω cm at 25°C) gets reduced when doped [29, 30]. According to Daniel and his group, noble metals tend to increase the electron-hole separation by acting as electron traps; they extend the light absorption into the visible range and improve surface electron excitation by size and shape dependent plasmon resonances excited by visible light; and/or modify the surface properties of TiO_2, Daniel et al [25].

Silver nanoparticles (Ag-NPs) are commonly used as a doping material because of their unique properties such as excellent conductivity, catalytic, optical, chemical durability, and antimicrobial properties [31, 32]. Ag-NPs can be synthesized using various methods; chemical and physical [32]. Balamurugan et al [32] reported that all these methods uses toxic and potentially hazardous materials, in some cases it may have adverse effects in medical applications, therefore researchers are developing and using green processes for the synthesis of Ag-NPs, which provides advancement over chemical and physical methods, due to cost-effective, environmentally friendly that requires no use of high pressure, energy, or temperature. Biological systems like plant extract, bacteria, and fungi are used as methods of synthesizing Ag-NPs, where Ag-NPs are synthesized from $AgNO_3$ solution of different molarities and various amounts of the plant extract at both ambient and elevated temperatures [32].

2.2.4 Doping TiO_2 system with sensitizers

This is another method used to extend light harvesting of TiO_2 into the visible region of the spectrum. The dye is physically adsorbed to the surface of the semiconductors through weak Van der Waals interaction. Therefore when the dye absorbs visible light; the excited state injects electrons into the semiconductor [4]. There are different sensitizers (catechol, porphyrins, phthalocyanines, etc.) that can be employed as sensitizers, but most of them are toxic and, they can easily undergo self-degradation process that makes them unsuitable for durable applications in photocatalysis [4].

2.3 Techniques used to synthesis metal oxide thin films

There are two approaches on how to fabricate metal oxide thin films, the physical and chemical approach. The physical methods are such as, physical vapor deposition (PVD), laser ablation, molecular beam epitaxy, thermal evaporation, sputtering and electron beam lithography, but they all have major drawback which is the failure in regulatory of particle size down to the nanometer scale [33]. The chemical methods contain gas phase and liquid phase deposition. The gas phase methods are such as chemical vapor deposition (CVD) and atomic layer epitaxy (ALE); while spray pyrolysis, sol gel process, molecular precursor methods are part of liquid phase methods. These chemical methods are mostly used; and they all offers a different set of advantages and disadvantages; and currently no method is proved to be more effective [2, 33, 34, 35].

2.3.1 Physical Methods

Physical vapor deposition

Physical vapor deposition is one of the methods that is widely used. Vapor deposition technique defines any procedure in which a solid submerged in a vapor becomes larger in mass due to transference of material from the vapor onto the solid surface, this deposition is mostly carried out in a chamber to control the vapor composition. When the vapor is created by physical means without chemical reactions, the process is called physical vapor deposition and when the vapor is created by chemical reactions, the process is called chemical vapor deposition [36]. Physical vapor deposition is a technique whereby physical processes, such as evaporation, sublimation or ionic impingement on a target, facilitate the transfer of atoms from a solid or molten source onto a substrate. Evaporation and sputtering are the two most widely used PVD methods for depositing films

The thermal evaporation method in a high vacuum system of ($3x10^{-6}$) torr using Edward coating unit model (E 306) from molybdenum boat, is used to deposit metal thin film on the glass substrate [36] and this method uses a Kilns Furnaces to carry out the thermal oxidation, whereby temperature is measured in Kelvin (K). This method results in structural and optical properties of metal oxides, and the structures are examined by the XRD method (X-ray diffraction), they use siemens x-ray diffractometer system, which records the intensity as a function of Bragg angle [36, 37].

2.3.2 Chemical Method

a) Sol-gel Method

This is the most widely used synthetic technique to fabricate metal/semiconductor composite thin film [2, 26, 31] because it is easy to control the chemical composition and low temperature synthesis that are very important for thin-film formation [38]. Marciello and his group, Marciello et al [33] define sol-gel method as a method that is "based on hydroxylation and condensation of molecular precursors in a solution, originating a sol of nanometric particles". Yuhas and Yang defines sol-gel method as a dip technique that is simple and low-cost, which requires no sophisticated specialized setup, where coating of substrate of large surface area can be easily obtained by this technique compared to that in physical evaporation techniques, spray pyrolysis and other methods [39].

The summary and features of sol-gel method for fabricating materials: it starts with a solution containing metal compounds (such as metal alkoxides and acetylacetonates as source of oxides) - metal compounds undergo hydrolysis and polycondensation at near room temperature, giving rise to sol, in which polymers or fine particles are dispersed; water as hydrolysis agent; alcohol as solvent; and acid or base as catalyst [35, 40]. There are different types of coating techniques that can be employed in sol-gel method, techniques such as dip coating, spin coating, laminar flow coating, printing, and spray coating [40]. When this gel films are heated to higher temperatures, organic constituents and residues are removed and this gives rise to microstructures of inorganic– inorganic composites or hybrids, and glasses and ceramics [35]. Using the X-ray diffraction (XRD) analysis of the films prepared by a conventional sol–gel process, Nagai and Sato

were able to show that the anatase phase appeared between 400 and 500°C and was not transformed to the rutile even when the thin film was heat-treated at 900°C and the irreversible phase transformation from anatase to rutile requires heat-treatment [35].

The gel's characteristics and structure can be easily controlled by fixing the hydroxylation and condensation conditions and the kinetic parameters of the growing process (parameters such as pH, temperature, nature and concentration of the salt precursors, solvent nature) [33]. This method can be used to fabricate many kinds of functional materials in different forms such as coating; organic/inorganic hybrids; fibers; thin films; materials with photonic and electronic functions; thermal and mechanical functions; and chemical, biochemical, and biomedical functions [2, 38, 40]. This technique permits good control of particle structure and size (with low particle size distributions), but the other hand it generate contamination by reaction products and posttreatment of the products [33] and it limits the incorporations of large amount of noble metals (Ag-NPs) up to 18 mol% due to Silver particles coalescing with each other into huge particles during sintering [25].

b) Molecular precursor method (MPM)

Nagai and Sato [35] defined the molecular precursor method (MPM) as a wet chemical process that is used for fabricating metal oxide and phosphate thin films and it requires heat treatment to eliminate organic ligands from metal complexes and alkylamine as the counter cation involved in spin-coated precursor films. Due to the results that were obtained using this method, which showed a great potential for the development of nanoscience and nanotechnology tools and materials, Nagai and Sato [35] emphasized

more on the importance of heat treatment. This method is based on the design of metal complexes in coating solutions with excellent stability, homogeneity, miscibility, coatability, which have many practical benefits [35].

Using this method, heat treatment of the precursor film between 400°C and 500°C, anatase phase appears; and is transformed to the rutile one between 500°C and 700°C [35]. What happens during the heat-treatment is the atom in the original tetragonal lattice of anatase can be rearranged into the rutile tetragonal lattice. Heat treatment is important; because it can be used produce silver nanoparticles by reducing Ag^{+} ions in the precursor film and forming well dispersed silver nanoparticles in the titania matrix [35].

The coating precursor solution is usually prepared by a reacting $Ti(OiPr)_4$ with ethylenediamine N,N,N′,N'tetraaceticacid (EDTA) under the presence of dibutylamine and hydrogen peroxide and the Silver precursor solution is easily prepared by simply dissolving the silver salt in ethanol, then the two precursor solutions can be mixed at different molar concentration to form a composite precursor solution [25, 31]. The composite precursor solution is then spin coated onto glass substrates producing metallic Ag-Nanoparticles/Titania (Ag NP/TiO_2) composite thin films [25]. This techniques allows various and unprecedentedly high amount of Silver particles, up to 80 mol% that are homogeneously distributed in titania matrix [25].

Sato and his group [4, 35] compared the TiO_2 fabricated by Molecular precursor methods and convectional sol gel methods, it was found that the crystallite sizes of the

TiO_2 thin films fabricated by MPM are generally smaller than those prepared by the conventional sol–gel method, the stability of the molecular precursor solution for Ti complex of EDTA is more stable than the SrO precursor solution containing a Sr complex of EDTA. Due to the above mentioned facts, "it was concluded that the MPM offers outstanding miscibility of the silver and titania precursor solutions, and is effective for overcoming the limitations in miscibility of the conventional sol-gel method and is necessary for fabricating Ag/TiO_2 composite thin films with amounts of $Ag \leq 80$ mol%" Likius et al [25].

2.4 Studies on Ag-nanoparticles/TiO_2

Due to their unique electronic, optical and magnetic properties, the surface plasmon resonance (SPR) of nanoparticles of noble metals such as gold, and silver has lately attracted much attention [41, 42, 43]. Kaimo et al [41, 44], described SPR as "originates from light (electromagnetic radiation) interacting with the free electrons of Ag-NPs, which results in the collective excitation oscillations that lead to strong enhancement of the local electromagnetic fields surrounding the nanoparticles". It is noted that when Ag-NP increases in content, than the intensity of SPR absorption peaks of the composite films increases. Jayraj et al [44] reported that in photovoltaics, plasmonics have improved the efficiencies of the devices due to its capability to increase the light scattering in thin film (far field effect), near field improvement by electric field and direct generation of charge carriers in semiconductor. It is found that the capacitance of plasmonic electrode is almost 45% higher than that of pure TiO_2 based electrode [44].

Studies done by Daniel [4] on heat treating Ag/TiO_2 thin films at different temperature; the thin films heated at 70°C, give an absorbance band at 410 nm which corresponds to the surface plasmon resonance of the silver nanoparticles; for the thin films fabricated at 250°C to 500°C, gives an absorbance of surface plasmon resonance shifted to longer wavelength with peak position at 540 nm. Due to the Localized Surface Plasmon Resonance (LSPR), electrons are promoted from the Silver nanoparticles to higher states in the band; the same electrons are then injected into the conduction band of TiO_2 provided they have sufficient energy; the photoexcited electrons then travel faster through the electrolyte to counter electrode producing a cathodic photocurrent [4, 45].

Daniel [4] further explained that at lower temperatures (70 - 400°C), Ag/TiO_2 shows resistance that varies from 9.6×10^{00} to 1.7×10^{00} Ω cm and at higher temperatures (400 - 800°C) resistance values of thin films are found to decrease from 1.7×10^{00} Ω - 1.4×10^{-4} Ω cm; the decrease in resistivity with heat treatment temperatures can be explained by: as silver particles size increases with increase heat treatment temperature it leads to a decrease in silver particles boundaries and hence the resistivity of the Ag/TiO_2 thin films [4].

In other studies proposed that the electrical resistivity changes strongly depends on the shape and size of the particles; and the quality of the particle boundary, which defines the percolation effects [46, 47]. The effect of the silver nanoparticles size in the Ag-NP/TiO_2 composite thin films on plasmon can be investigated by Transmission Electron Microscopy (TEM).

Studies on the photocurrent density mechanism of noble metal/TiO_2 composites have been focused on the details of the photo-induced electron transfer from the conduction band of TiO_2 to noble metals for improving the Vis-response activity of TiO_2 at lower Ag mol% (3-6%) [8, 17, 29]. Zhao et al. [29] reported an increase in the anodic photocurrent in the visible region for Ag particle dispersed electrodes, which was thought to result from the surface plasma resonance (SPR) of the metal nanoparticles. Doping TiO_2 matrix with Ag-NPs has led to nearly 45% improvement in the photocurrent while 15% enhancement in the fill factor. It is evident that doping TiO_2 (semiconductor) with metallic particles (Ag-NPs) leads to enhancement in electron density leading to better charge mobility.

Other application of Ag-NP/TiO_2, reported by Lin [48] reported that Ag-TiO_2/functional filter can be applied to remove the odorous compounds (such as volatile organic compounds, acetic acid, and dimethyl sulfide) from the industries, because these odorous compounds exhausts would persecute residents' health and lower the environmental quality.

2.5 Dye sensitizers

Dye sensitizers are considered to be the key role in the emerging of high performance of Dye Sensitizers Solar Cells. They should have requirements such as strong absorption in the visible light spectrum to the near infrared, they should be able to bound on the semiconductor through the chemical group and that they should be able to inject electrons into a semiconductor surface [49].

2.5.1 Inorganic dye sensitizers

The most commonly used inorganic dye is the ruthenium based dyes, ruthenium (II) complex containing polypyridine ligands, have been investigated by many researchers, this is due to their high catalytic performance in homogenous catalysis and high solar power conversion efficiency [10, 50]. The dinuclear ruthenium (II) dye sensitizer that was synthesized by Cheng et al [10] was used on the photocatalytic water splitting for hydrogen (H_2) production over TiO_2 (P25) under visible light ($\lambda \geq 400$ nm) irradiation, this demonstrated a good stability and sufficient reproducibility for over 6 hours. The photosensitization ability of the sensitizer was due to its conjugation system, larger molecular area, TiO_2 linkage mode and the antenna effect. Ryan [11] reported that the most efficient dye sensitizers demonstrated to date is based on ruthenium dyes developed by the Grätzel group: N3, N719 and 'black' dye.

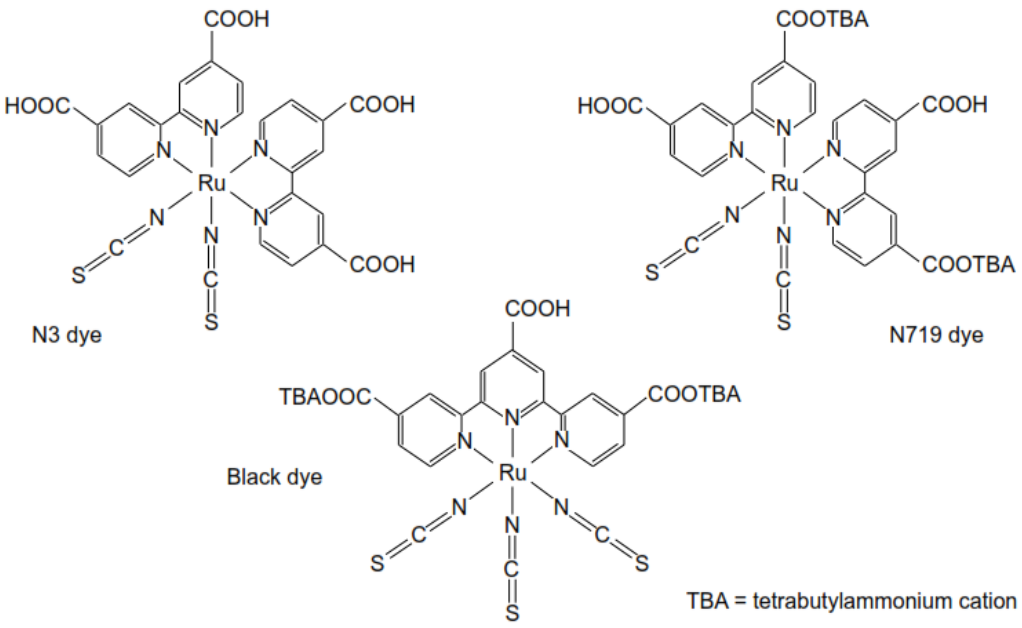

Figure 3 Structures of the ruthenium – based dyes N3, N719 and 'black' dye [51, 52].

2.5.2 Organic dye sensitizers

Organic sensitizers have been used to harvest a large amount of sunlight ranging from the UV region to the near infrared region of the spectrum leading to power conversion efficiencies of up to 10.65% to 13.00% for metal free organic sensitizers [53, 54].The metal free organic dyes have much stronger light harvesting ability than the metal complexes (inorganic dyes), this is due to its outstanding higher molar extinction coefficients [53]. They can be synthesized and purified in an easier and more economical way than those of Ru-dyes. Examples of organic dyes are B18, BTD-R, Phthalocyanine, CPTD-R [55], zinc porphyrin dye, Anthraquinone and Co(II/III) tris(bipyridine) [54].

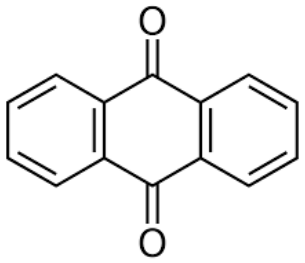

a) Anthraquinone

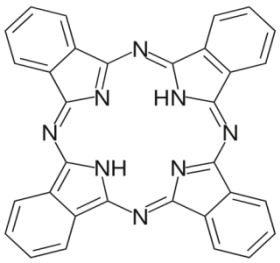

b) Phthalocyanine

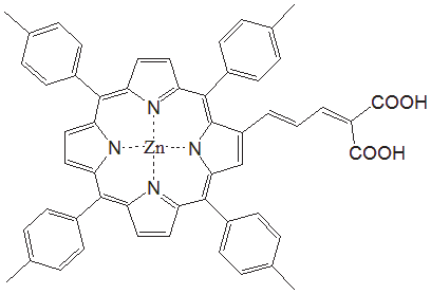

c) Zinc porphyrin

Figure 4 Structures of the metal free organic dyes [54, 55].

2.5.3 Natural dye sensitizers

Natural dyes are simply extracted from fruits, plants and leaves; they are used as sensitizers, where they serve as photons absorber from sunlight. There are different natural sensitizers; chlorophyll which is extracted from green leaves; anthocyanins mainly from fruits, which give color to fruits and plants (red-purple), have light absorbing in the range of 520-550 nm wavelengths; tannin, betalain (extracted from a variety of vegetable species typical of mediterranean, tropical and subtropical areas); roselle and carotene are responsible for the orange color of the carrot and other colors of many other fruits and vegetables [49, 56]. To date chlorophyll, raw anthocyanins and betalain dyes are the most effective natural sensitizers, resulting in the generation of monochromatic photon to current conversion yields exceeding 60% [56].

Table 1 Comparison of the chlorophyll and roselle extract sensitized solar cell [15, 57].

	Chlorophyll	**Roselle extract sensitized solar cell**
Open circuit voltage (V_{OC})	0.561 V	0.470 V
Short circuit current (I_{SC})	0.402 mA/cm^2	0.180 mA/cm^2
Fill factor (FF)	41.65%	55.2%
Efficiency	0.094%	0.046%

a) Chlorophyll dyes

Chlorophyll is a compound that is known as a chelate, meaning it contains of a central metal ion (Magnesium) bonded to a large organic molecule, composed of carbon, hydrogen, and other elements such as oxygen and nitrogen [15]. Chlorophyll is a green pigment, found in cyanobacteria and the chloroplasts of algae and plants. Apart from coloring chlorophyll has another important role. The chlorophyll function is to directly absorb light from the sun; transfer the light energy by resonance energy transfer to a specific chlorophyll pair in the reaction center of the photosystems; and finally performing charge separation [15].

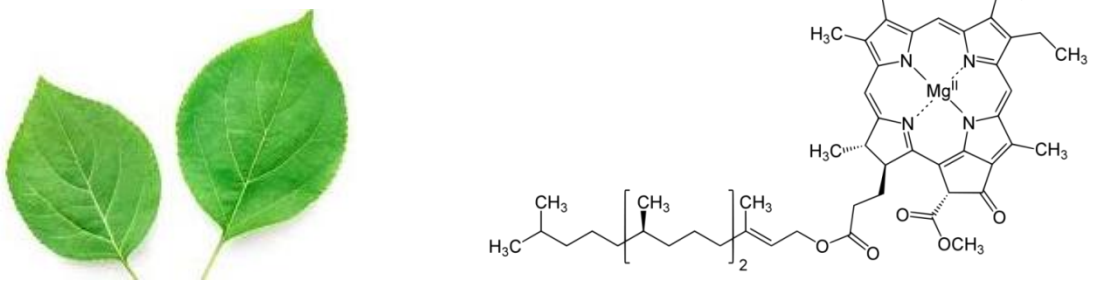

a) b)

Figure 5 a) plant leaves and b) a structure of chlorophyll.

Chlorophyll helps to trap solar energy; when chlorophyll absorbs energy from sunlight, an electron in the chlorophyll molecule is excited from a lower to a higher energy state. The excited electron is more easily transferred to another molecule. Chlorophyll absorbs light from red to violet wavelengths and obtains its color by reflecting the green wavelength, because of its ability to absorb photon from sunlight, chlorophyll can be used as a dye sensitizer and it have a light harvesting invisible light spectrum [49]. From

the UV-Vis absorption spectrum, it has been known that chlorophyll extracted with distilled water has the broader region of the visible light spectrum in the range of 400 to 720 nm compared to chlorophyll extracted with ethanol [49]. The lowest bandgap of dye also presented by extracted the chlorophyll with distilled water with 1.83 eV and the absorption coefficient of 1.59 Km^{-1} [49]. The photo electrochemical parameter for solar cell by using chlorophyll extracted with deionized water solvent showed the open circuit voltage of 440 mV, current short circuit of 0.35 mA and a fill factor of 0.49 [49]. Chlorophyll as a green dye is available commercially and it can be used in processed foods, toothpaste, soaps and cosmetics.

b) Anthocyanin dyes

Anthocyanin is a class of flavonoids (synthesized via the phenylpropanoid pathway) that depends on their pH and they are responsible for the red and purple coloration of many fruits and flowers; it has a positive absorption in the 580–700 nm region(s) on the spectrum and shows intense bleaching red shifted [57]. Some food plants that contain anthocyanins are the blueberry, raspberry, black rice, and black soybean. Anthocyanins are approved for use as food colorants and they can be used as pH indicators, that is because of their color changes with pH; when they are red or pink in acidic solutions, the pH < 7; when the dyes are purple in neutral solutions, the pH ~ 7; for greenish-yellow in alkaline solutions, the pH > 7; and they are colorless in very alkaline solutions, where the pigment is completely reduced [58].

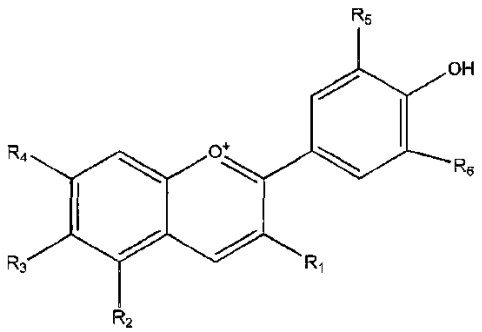

Figure 6 Chemical structure of anthocyanin [58].

c) Betalain dyes

Betalain dyes are classified as a class of red and yellow indole-derived pigments found in plants of the Caryophyllales, where they replace anthocyanin pigments [56]. These dyes occurs in petals of flowers, fruits, leaves, beets, stems, and roots of plants and can also occur in some higher order fungi. It is thought that betalains are related to anthocyanins, both are water-soluble pigments found in the vacuoles of plant cells, however structurally and chemically they differ, for example betalains contain nitrogen (N) and anthocyanin do not have nitrogen; betalains are not flavonoids; and the two have never been found in the same plant together [59].

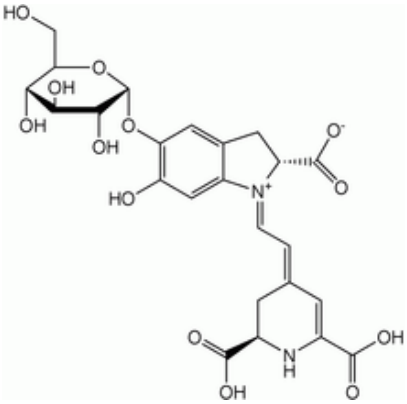

Figure 7 Chemical structure of betalain [59].

Betalains are also called beetroot red after the fact that it may be extracted from red beet roots; they are known to be aromatic indole derivatives that are synthesized from tyrosine; their synthesis is promoted by light [59]. Betalains are used as coloring agents in food and their color is sensitive to pH. Betalain absorb light in the visible region between 476 nm and 600 nm, which suggest that it is good for solar cells [60]. Betalain dye structure has the COOH functional group, which is used to bind the dye to the molecule of TiO_2 surface [60].

2.5.4 Comparison of synthetic and natural dye

Table 2: Comparison of the synthetic dye (inorganic and organic dye) and natural dye [11, 15, 54, 60].

Parameter	**Sensitizer**	
	Synthetic dye	**Natural dye**
Cost	High cost	Low cost
Environmental effects	Bad effects	Less effects
Stability	Slowly degrade in the presence of sunlight therefore long life of DSSC	Degradation of natural dye in the presence of sunlight radiation results stability problem in DSSC
Absorption on solar spectrum	Absorption up to 800 nm	Visible region (400 – 700 nm)
Efficiency	High efficiency (10% -	Low efficiency (0.02– 0.094%)

	13%)	
Availability	No long term availability	100% available
Fabrication process	Requires multi procedures (making synthetic dye production very expensive)	Requires simple and direct chemical procedures, making natural dye production less expensive

2.5.5 Properties enhancement of dye sensitizers

Dye sensitizer's performance can also be enhanced by silver nanoparticles, because of its Surface Plasmon Resonance; this unique property can broaden the dye spectral absorption range with the long wavelength absorption edge shifting from 680 nm to the infrared region beyond 800 nm, this enhancement happens when SPR of Ag-NPs interacts with the dye, enhancing dye absorption resulted in more charge carrier generation [41].

2.6 Characterization of the thin films

2.6.1 UV-vis spectrophotometer

UV-vis spectrophotometry refers to absorption spectroscopy or reflectance spectroscopy in the ultraviolet-visible spectral region, meaning it uses light in the visible and adjacent (near-UV and near-infrared [NIR]) ranges. Harris defined spectroscopy as the study of molecular structure and dynamics through the absorption, emission and scattering of light, which is convenient to describe light in terms of both particles and waves [61]. The absorption spectroscopy uses electromagnetic radiations between 190 nm to 800 nm and

is divided into the ultraviolet (UV, 190-400 nm) and visible (Vis, 400-800 nm) regions [62].

Spectroscopy instruments requires a radiation source (varies with the wavelength range for which it is used), a wavelength selection device such as a monochromator, a sample holder (transparent to the radiation range being studied), a detector (to measure the intensity of the radiation and convert it to a signal) and a readout (to display and process the signal from the detector) [63].

The principle of absorption: to determine the absorbance, the Beer Lambert's law is used. This law states that; the greater the number of molecules that absorb light of a given wavelength, the greater the extent of light absorption and higher the peak intensity in absorption spectrum; and if there are only a few molecules that absorb radiation, the total absorption of energy is less and consequently lower intensity peak is observed [62].
Beer- Lambert law:

$$A = \log\left(\frac{Io}{I}\right) = \varepsilon cL$$

Where I_o = Intensity of the incident light (or the light intensity passing through a reference cell), I = Intensity of light transmitted through the sample solution, c = concentration of the solute in mol l^{-1}, L = path length of the sample in cm and ε = molar absorptivity or the molar extinction coefficient of the substance whose light absorption is under investigation. The ratio I / I_o is known as transmittance T and the logarithm of the inverse ratio I_o / I is known as the absorbance A. This means when the radiation passes through a sample, the amount of light absorbed or transmitted is an exponential function

of the molecular concentration of the solute and also a function of length of the path of radiation through the sample.

Nature of the electronic transition: when the molecule is exposed to light, The molecule can absorb radiation and move from the lowest energy state to a higher energy state, when the molecule becomes excited, an outer shell electron moves to an orbital of higher energy (this process of moving electrons to higher energy state is called electronic excitation) [63]. For radiation to cause electronic excitation, it must be in the visible or Uv region of the electromagnetic spectrum. Generally, the most probable transition is from highest occupied molecular orbital (HOMO) to lowest unoccupied molecular orbital (LUMO). The frequency absorbed or emitted by a molecule and the energy of radiation are related by:

$$\Delta E = h\nu$$

The actual amount of energy required depends on the difference in energy between the ground state E_o and the excited state E_1 of the electron [63]. The relationship is described by:

$$\Delta E = E_1 - E_o = h\nu$$

Since electrons are transferred from low energy (atomic or molecular orbitals) to high energy (atomic or molecular orbitals) in the UV-vis spectroscopy, when the materials are irradiated with light, sometimes it is called electronic spectroscopy [64]. There are three distinct types of electrons involved in valence electron transitions in molecule. The first are the electron involved in the single bond, for example those between carbon and

hydrogen in alkanes, these bonds are called sigma (σ) bonds [63]. The amount of energy required to excite electrons in σ bonds are usually more than UV photons of wavelengths > 200nm possess, for this reason, alkanes (such as hexane) and other saturated compounds (compounds with only one single bonds) do not absorb UV radiation [65].

The second are electrons which involved in the double or triple (unsaturated) bonds, these bonds involve a pi (π) bond (for example alkenes, alkynes, conjugated olefins and aromatic compounds [63]. Electrons in π bonds are excited relatively easily; these compounds commonly absorb in the UV or visible region [65]. The last type of electron are the ones that are not involved in the bonding between atoms (electron in the molecule), these are called n electrons, for nonbonding electrons [65]. Examples of compounds that contain n electrons are nitrogen, oxygen, sulphur or halogens. Because n electrons are usually excited by UV or visible radiation, many compounds that contain n absorbs UV/Vis radiation.

Since its development in the 1950's the UV-Visible Spectrophotometer has progressed into an accurate and reliable analytical tool and it has become one of the most utilized instrument in today's scientific laboratory [68]. This technique is a mature and well established analytical technique used extensively in many industry sectors including environmental analysis; pharmaceutical testing; and food and beverage production [68]. UV-VIS spectroscopy is routinely used in analytical chemistry for the quantitative determination of different analytes, such as transition metal ions, highly conjugated organic compounds, and biological macromolecules, in organic molecules to determine the impurities and in nanotechnology to determine the size, absorbance and band gap of

the nanoparticle [61, 63, 66]. In this research, this technique was used to study the absorbance of the composite thin films and to determine the band gap of the fabricated thin films

2.6.2 Fourier-transform infrared (FTIR) spectrometers

Fourier-transform infrared spectrometer is defined as a method used to get an infrared spectrum of absorption or emission of a solid, liquid or gas [67]. The Infrared region is divided into near-infrared region (12800 ~ 4000 cm^{-1}), mid-infrared region (4000 ~ 200 cm^{-1}) and far-infrared region (50 ~ 1000 cm^{-1}) [68]. When a sample is exposed to Infrared (IR) radiation, the radiation pass through a sample, some radiation is absorbed and some is transmitted through a sample; this results in a molecular "fingerprint" spectrum (sometimes called the molecular vibrational spectrum) of the sample [67, 68]. A FTIR spectrometer consists of a source, interferometer, sample compartment, detector, amplifier, A/D convertor, and a computer; whereby the source generates radiation which goes through a sample in the interferometer and reaches the detector; the signal is then amplified and converted to digital signal by the amplifier and analog-to-digital converter, respectively [68]. Finally, the signal is then transferred to a computer in which Fourier transform is carried out.

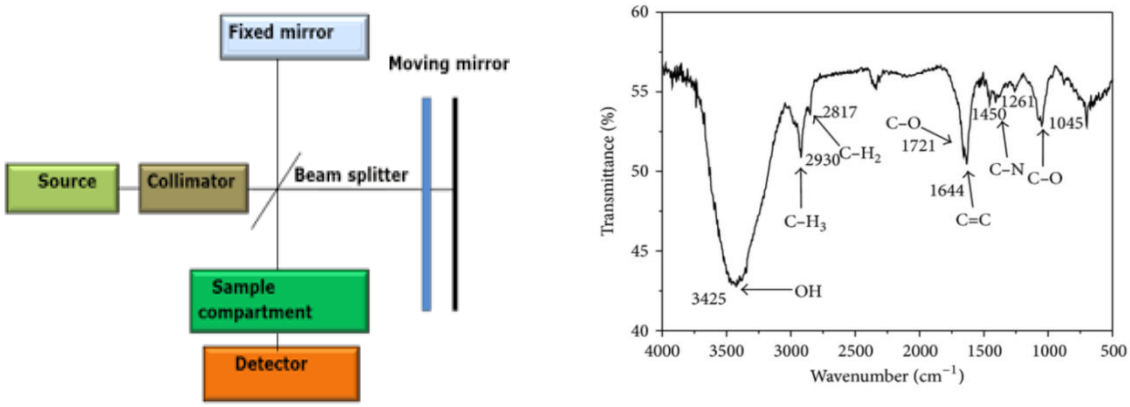

a) b)

Figure 8 Represents a) block diagram of an FTIR spectrometer and b) FTIR spectra of chlorophyll dye [68].

This technique can be used by analysts to identify or quantify materials, since molecules exhibit specific IR fingerprints. FTIR technique can be applied in many fields, such as: organic synthesis, polymer science, petrochemical engineering, pharmaceutical industry and food analysis. FTIR can provide information such as [67, 68]:

- The identification of an unknown.
- Quantitative information, such as additives or contaminants.
- Kinetic information through the growth or decay of infrared absorptions.
- More complex information when coupled with other devices such as Rheometry.

In this study, this technique was used to confirm whether the dye extracts from the mopane leaves and the makalani leaves are indeed chlorophyll dye.

2.6.3 Band Gap

Band gap is the distance between the valence band of electrons and the conduction band; the band gap represents the minimum energy that is required to excite an electron up to a state in the conduction band where it can participate in conduction. The lower energy level is the valence band, and thus if a gap exists between this level and the higher energy conduction band, energy must be input for electrons to become free.

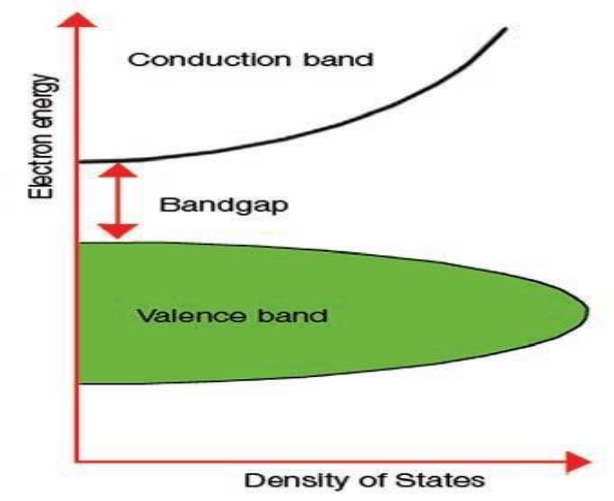

Figure 9 Band gap diagram [69].

For the conductor materials the valence band overlaps with the conduction band, so there is no band gap, the overlap causes the electrons to move freely from valence band into the conduction band and participate in conduction; and for the semiconductors, the gap is small enough that it can be bridged by some sort of excitation (in terms of photovoltaic cell it can be from the from the Sun), the gap is basically some size "in-between" that of a conductor or insulator [69]. What happen is: the electron from an atom close by can occupy this space, generating a chain reaction of holes and electron

movement that creates current and a small amount of doping material can drastically increase the conductivity of this material [70]. For the insulator materials, they have large band gap energy, which means that no electrons can reach the conduction band from the valence band. Band gap is one of the properties used to determine whether the thin film can respond to the visible light [71].

CHAPTER 3: RESEARCH METHODS

3.1 Research design

Figure 10 below display the design for the research project, where two precursor solutions (titanium precursor solution and silver precursor solution) were used to fabricated composite thin films, which were then immersed in chlorophyll dye that was extracted from plant leaves using methanol as a solvent extract.

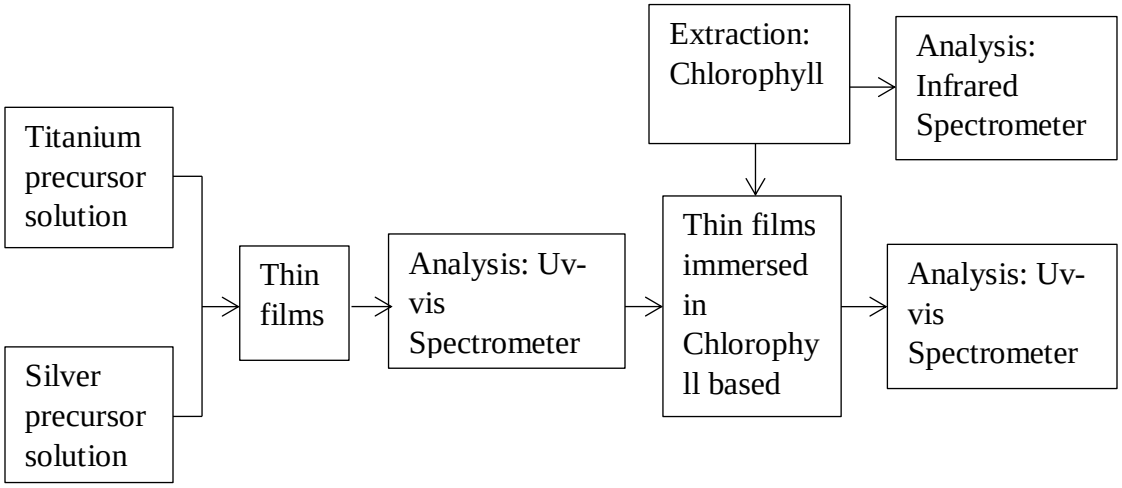

Figure 10 Flow diagram showing project research design.

3.2 Procedures

3.2.1 Extraction of Chlorophyll as dye sensitizers from dry leaves

Chlorophyll dye was extracted using the procedures reported by Huizhi et al [72] and Mahmoud et al [60]. Dry leaves were obtained from the Mopane tree, traditionally called Omusati and scientifically called *Colophospermum Mopane* shown in figure 11 (a); and the Makalani Palm tree, traditionally called Omulunga and scientifically called *Hyphaene petersiana* shown in figure 11 (b); all from Omusati region, in Northern

Namibia. All leaves were blended to fine powder and 20 g of powdered dry leaves were put in different beakers and 200 ml of methanol was added to each beaker. All samples were left in the cupboard for a week. Samples were filtered and the filtrates were stored in the cupboard, for analysis and future use, as shown in figure 11 (c).

a) Mopane tree leaves

b) Makalani tree leaves

c) Chlorophyll dye

Figure 11 a) and b) the source of chlorophyll and c) the dyes extracts.

3.2.2 Preparation of the Precursor Solutions

The precursor solutions was prepared using the procedures reported by Daniel et al [31], where precursor solution of Ti^{4+} containing the Ti^{4+} complex of EDTA and the precursor solution of Ag containing silver acetate were obtained as illustrated in scheme 3.1 and 3.2, respectively.

Titania precursor solution

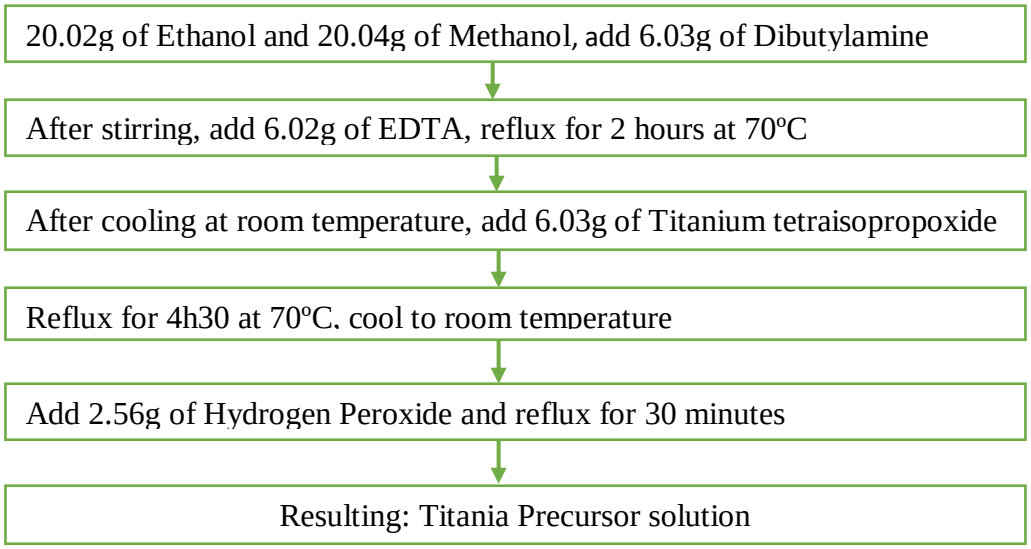

Scheme 3.1 Preparation procedures of the precursor solution of Titania containing a Ti^{4+} complex of EDTA.

Silver precursor method

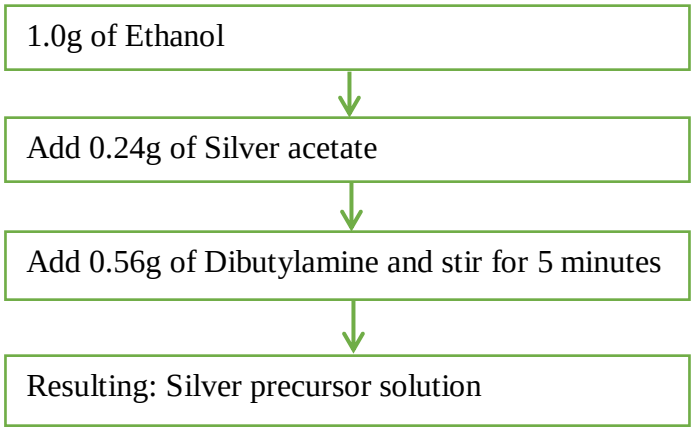

Scheme 3.2 Preparation procedures of the precursor solution of Silver containing silver acetate.

3.2.3 Fabrication of Ag-NP/TiO_2 composite thin films

Cleaning procedures for the glass substrates: the glass (1.5 cm × 2.5 cm) substrates were cleaned using procedures reported by Karabay et al [2]; they were first washed with detergent and water for 30 minutes; followed by 5 minutes of acetone; and finally 30 minutes of distilled water all in ultrasonic bath. The substrates were dried at room temperature.

The silver precursor solution that was prepared was immediately used to dope Ti^{4+} precursor solution to fabricate Ag-NP/TiO_2 composite thin films, by adjusting the silver solution concentration (25, 50 and 75mol %). The silver precursor solution was immediately used because silver is very sensitive to light, it actually reacts with light. The doped and undoped solutions were spin coated on the quartz glass at double step mode; Step 1 used a speed of 500 rpm for 5 seconds; and step 2 used a speed of 2000 rpm for 30 seconds. The spin coated thin films were heated at 550°C for 30 minutes and they were cooled for analysis.

3.2.4 Fabrication of Ag-NP/TiO_2/Chlorophyll dye sensitizer composite thin films

After analysis of the Ag-NP/TiO_2 composite thin films, they were then immersed in solutions of chlorophyll dye sensitizer for 48 hours for the dye to be adsorbed on the thin films [73, 74, 75, 76]. The Ag-NP/TiO_2/Chlorophyll dye sensitizer thin films were dried in the dark cupboard for 24 hours and after drying they were analyzed.

3.3 Optical properties of the thin films

3.3.1 Absorption properties of the fabricated thin films and IR spectra of extracted Chlorophyll

UV-VIS Spectrophotometer (PerkinElmer machine, using scan Lambda 35 software) was used to study the absorption properties of the fabricated thin films. Fourier-transform infrared (FTIR) spectrometer (Nicolet 380 FT-IR Spectrometer) was used to produce infrared spectra, to identify chemical compounds in the dye solution.

3.3.2 Calculation of the optical band gap

Optical band gap, sometimes called the energy gap, which generally refers to the energy difference between the top of the valence band and the bottom of the conduction band. The absorbance, proportionality constant and the photon energy was obtained from the UV-VIS Spectrophotometer analysis spectra, which was used to calculate the optical band gap (E_g) of thin films using the Tauc's expression:

$$\alpha = \frac{A(E_{phot} - E_g)n}{E_{phot}},$$

where E_{phot} is photon energy, A is a proportionality constant, α is the absorption coefficient at wavelength λ (nm), and n is equal to 0.5 by considering values for the direct mode of transition [4].

CHAPTER 4: RESULTS AND DISCUSSIONS

4.1 The fabricated Ag-NP/TiO_2 composite thin films

Five composite thin films were fabricated at different concentrations on quartz glass, varying the silver (Ag) molar concentrations [0 (pure TiO_2), 25, 50, 75 and 100 (pure 100 Ag) mol%]. Figure 12 below shows the resultant fabricated thin films. The thin films were sintered at 550°C that is to fasten the deposited Ag-nanoparticles and most importantly to eliminate organic ligands from metal complexes. The composite thin films color varies as the concentration of silver changed, this is due to their unique property surface plasmon oscillations [4].

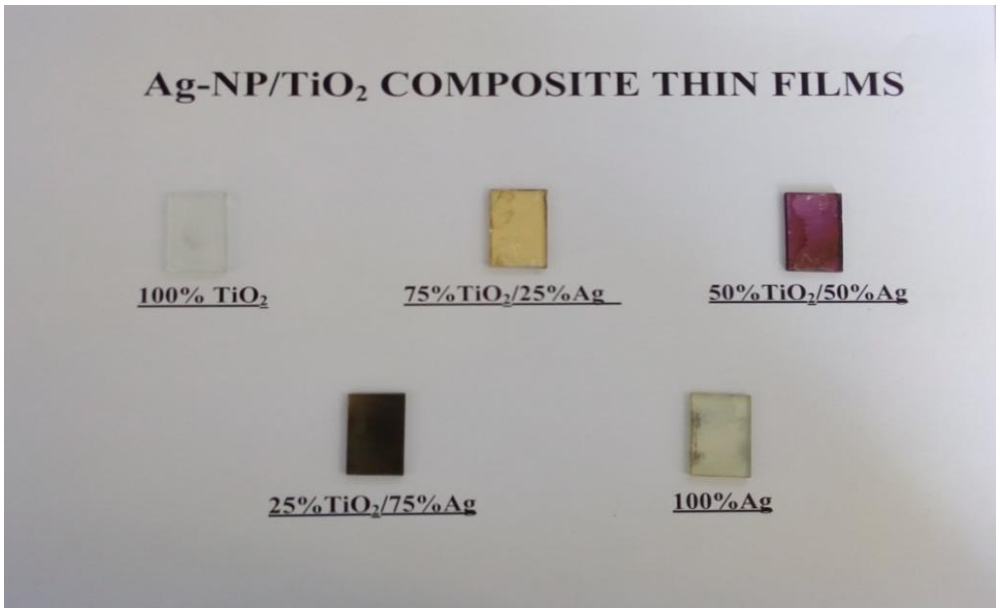

Figure 12 The fabricated composite thin films

4.2 The fabricated of Ag-NP/TiO_2/Chlorophyll dye sensitizer composites thin films

The Ag-NP/TiO_2 composites thin films that were fabricated were immersed in dye solutions. Figure 13 shows the resultant Ag-NP/TiO_2/Chlorophyll composite thin films.

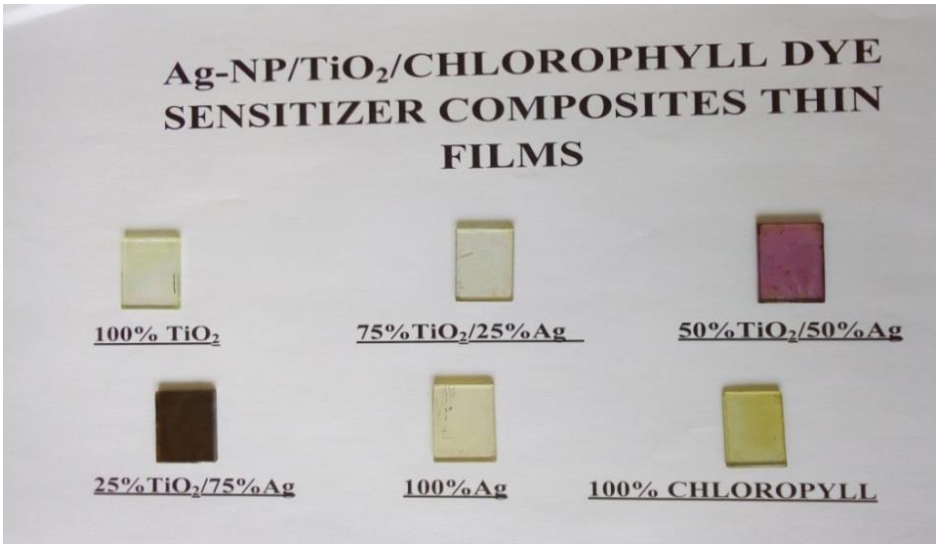

Figure 13 Ag-NP/TiO_2/Chlorophyll composite thin films.

4.3 Infrared spectra for the extracted Chlorophyll dyes

IR spectra can used to identify unknown compounds in samples using their functional groups and it can also be used to obtain quantitative information, such as additives or contaminants on sample, but in this study it was used to confirm whether the dye extracts that were extracted from the Mopane and Makalani leaves was indeed chlorophyll. The spectra obtained were compared to that of the library spectrum of chlorophyll. Figure 14 and 15 below shows the infrared spectra of Chlorophyll dyes extracted from Mopane and Makalani leaves.

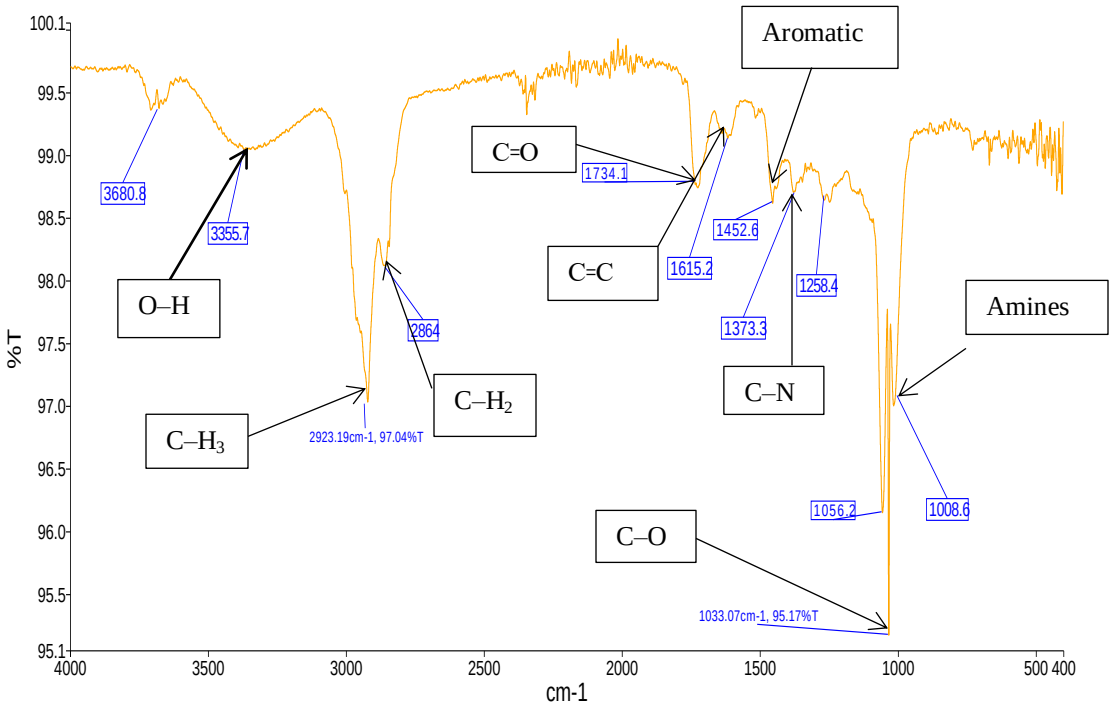

Figure 14 Infrared spectrum of the Chlorophyll dye extracted from Mopane dye.

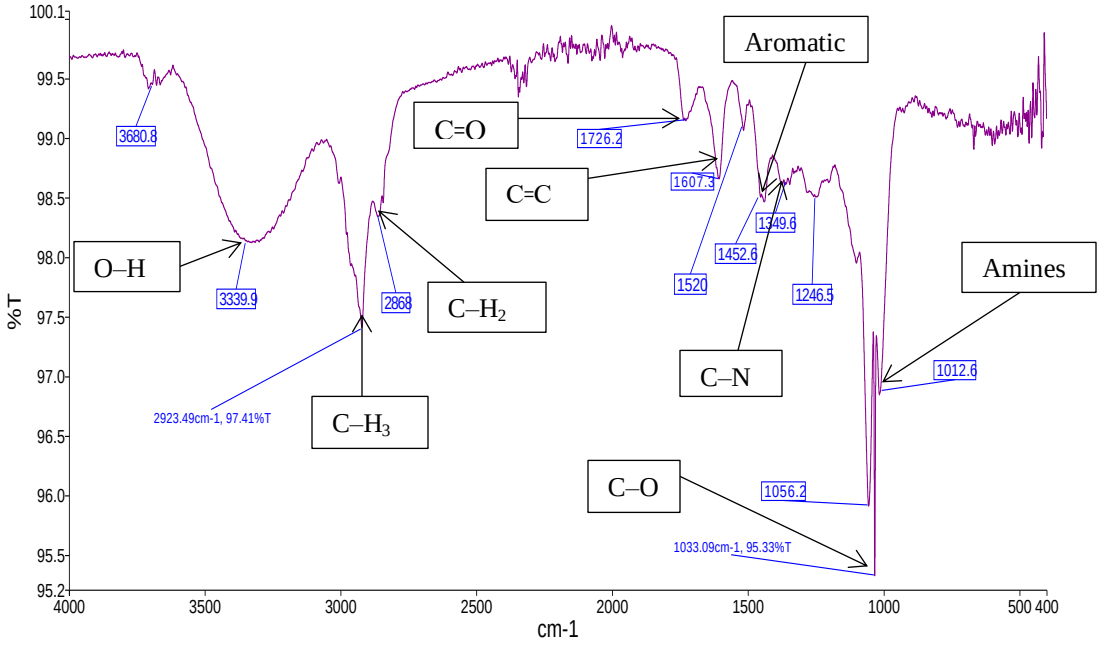

Figure 15 Infrared spectrum of the Chlorophyll dye extracted from Makalani dye.

Both FTIR spectra of dye extracts from different leaves (Mopane and Makalani leave) showed the same functional group. The FTIR spectra showed different functional groups that appears in the wavelength range of 4000 – 1000 cm^{-1} which is the mid-infrared region (4000 ~ 200 cm^{-1}); with a sharper peak of C–O appearing at 1033.09 cm^{-1} and a broader peak of O–H at 3339.9 cm^{-1} and the lowest peak intensity of Amines appearing at 1012.6 cm^{-1}.

The spectra showed also different functional of $C–H_3$, $C–H_2$, C=O, C=C, aromatic and C–N appearing at 2923.49, 2864, 1734.1, 1615.2, 1452.6, and 1373.3 cm^{-1} respectively. The results obtained in these spectra are consistent with the work reported by Al-Alwani and his group [60].Comparing these FTIR spectra to the one of the library spectrum of chlorophyll, they have the similar functional groups, using this observation and data obtained, it is safe to say that the dye extracted and used in this research is indeed chlorophyll. This data can be validated using the absorption peaks of chlorophyll that are reported in literatures [14, 63] instead of using nuclear magnetic resonance (NMR).

4.4 Characterization of the optical properties

4.4.1 UV-Vis absorption spectra of Chlorophyll dye sensitizers

Figure 16 displays the UV-Vis absorption spectra of Chlorophyll dye extracts from different plant leaves (Mopane and Makalani leaves), using methanol as a solvent. Chlorophyll absorbs certain wavelengths of light strongly within the visible light spectrum. Both dyes extracted from Mopane and Makalani leaves showed two strong absorption peaks located in the visible region. The first absorbance peak is in the range

of 400 nm to 440 nm with peak absorbance maximum at ~425 nm, and the second absorbance peak is in the range of 640 nm to 680 nm with peak absorbance maximum at ~665 nm, this is consistent with the results that was reported by Syafinar et al [14] and Al-Alwani et al [60]. This confirmed that chlorophyll dyes were indeed extracted.

The absorption peak at 425 nm proves that chlorophyll absorbs light in the blue region (short wavelength); the absorption peak at 665 nm proves that chlorophyll absorbs light in the red region (long wavelength) of the visible light spectrum; reflecting light in the green region (large drop region between the blue region and the red region) making the plant leaves to appear green [14].

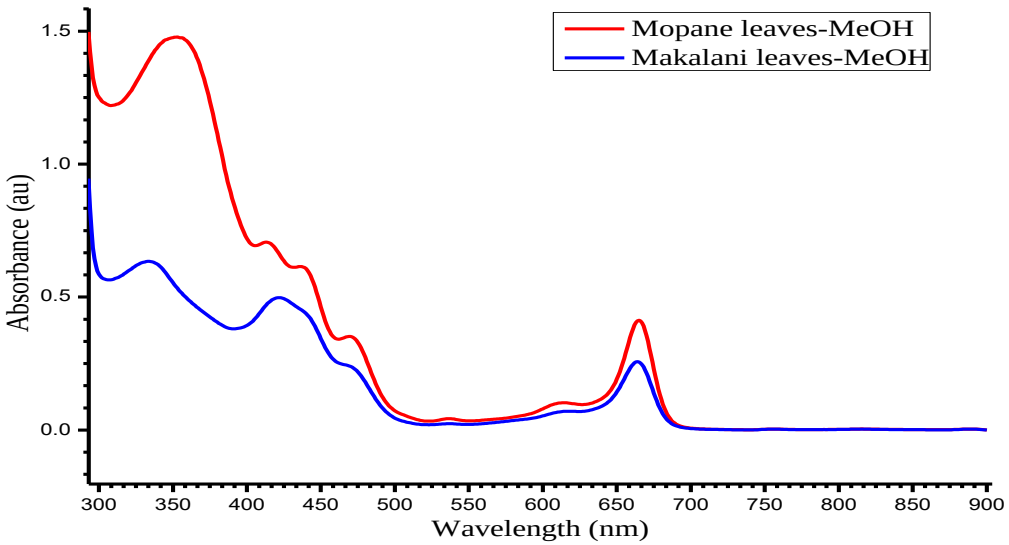

Figure 16 UV-Vis absorption spectra of Chlorophyll dye sensitizers.

4.4.2 UV-vis absorption spectra of Ag-NP/TiO_2 composites thin films

The optical properties of the TiO_2, Ag-NP and Ag-NP/TiO_2 thin films were studied using UV-vis spectroscopy. The absorption spectra of these thin films are presented in figure 17 below. The absorption of the entire visible region for thin films with Ag-NPs was stronger than that for the thin film without Ag-NPs at 410 nm, which could be the product of two distinct effects; firstly the absorption peak attributed to the surface plasmon resonance (SPR) of metallic silver nanoparticles in the TiO_2 matrix was red-shifted and broadened due to the high refractive index of anatase TiO_2 [31, 34, 77]; and secondly a well-separated Ag-NPs with wide range of size and shape exhibited a broad band, improving the absorption throughout the entire visible region [78]. Red-shift, sometimes called bathochromic shift means a change in absorbance to a longer wavelength (λ) [77].

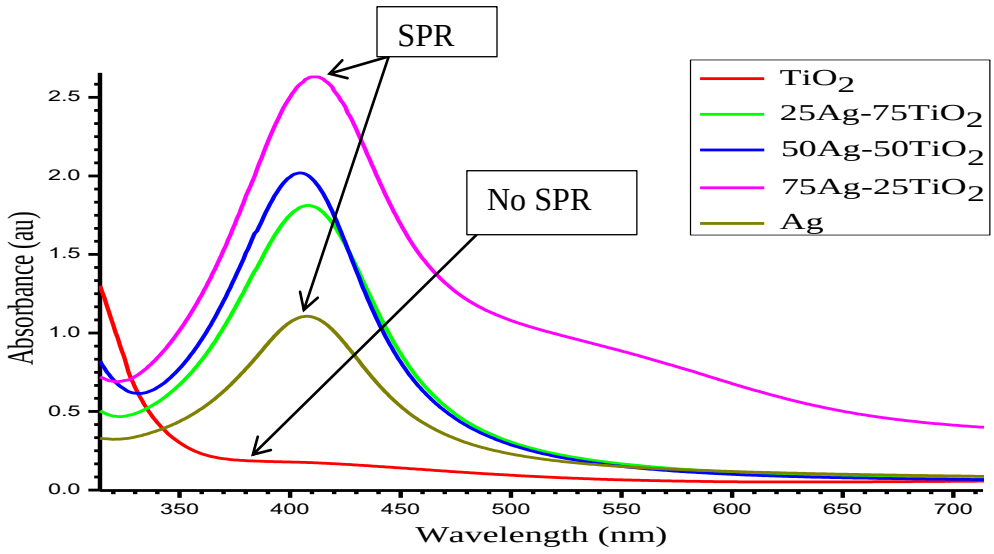

Figure 17 UV-Vis absorption spectra of Ag-NP/TiO_2 composite thin films.

The 100% TiO_2 thin film did not show any absorbance peak in the visible region because of its wide band gap, which remains confined to the UV-region. The 100% Ag thin film showed an absorbance peak in the range of 360 nm to 450 nm, with absorbance peak maximum at ~410 nm (in the visible region) which was due to the surface plasmon resonance (SPR) and hence confirming the present of silver nanoparticles [31]. Due to the SPR, it results in strong enhancement of the local electromagnetic fields surrounding the nanoparticles [30].

The 50%Ag-NP/50%TiO_2 and 25%Ag-NP/75%TiO_2 composite thin films both showed absorption peaks in the range of 350 nm to 460 nm with absorbance peak maxima at ~410 nm; this means that the silver nanoparticles have influenced the absorbance in the visible region due to its unique property the surface plasmon resonance, confirming the red shift of the TiO_2 matrix. The 75%Ag-NP/25%TiO_2 composite thin films firstly showed tremendous increase in absorbance with a distinctive absorption peak in the range of 350 nm to 450 nm, with absorbance peak at ~415 nm; and secondly showed a broader band at 550 nm. The SPR peak is increasing with increase Ag-NPs in titania matrix, this property enhanced the absorption and the photo responsive properties of the TiO_2 in the visible region [80].

4.4.3 Uv-vis absorption spectra of Ag-NP/TiO_2/Chlorophyll dye sensitizer composites thin films

a) Thin films immersed in chlorophyll dye extracted from Mopane leaves

Figure 18 presents the UV-vis absorption spectra of composite thin films (Ag-NP/TiO_2/Chlorophyll dye), that were immersed in the chlorophyll dye extracted from Mopane tree leaves, using methanol as a solvent. The TiO_2, Ag-NPs and Ag-NP/TiO_2 thin films showed tremendous absorption enhancement when the chlorophyll was adsorbed onto them, which can be explained by metal-to-ligand charge transfer, through which the photoelectric charge is injected into the TiO_2 [11,10] and surface plasmon resonance [77], notably some peaks were seen to red shift.

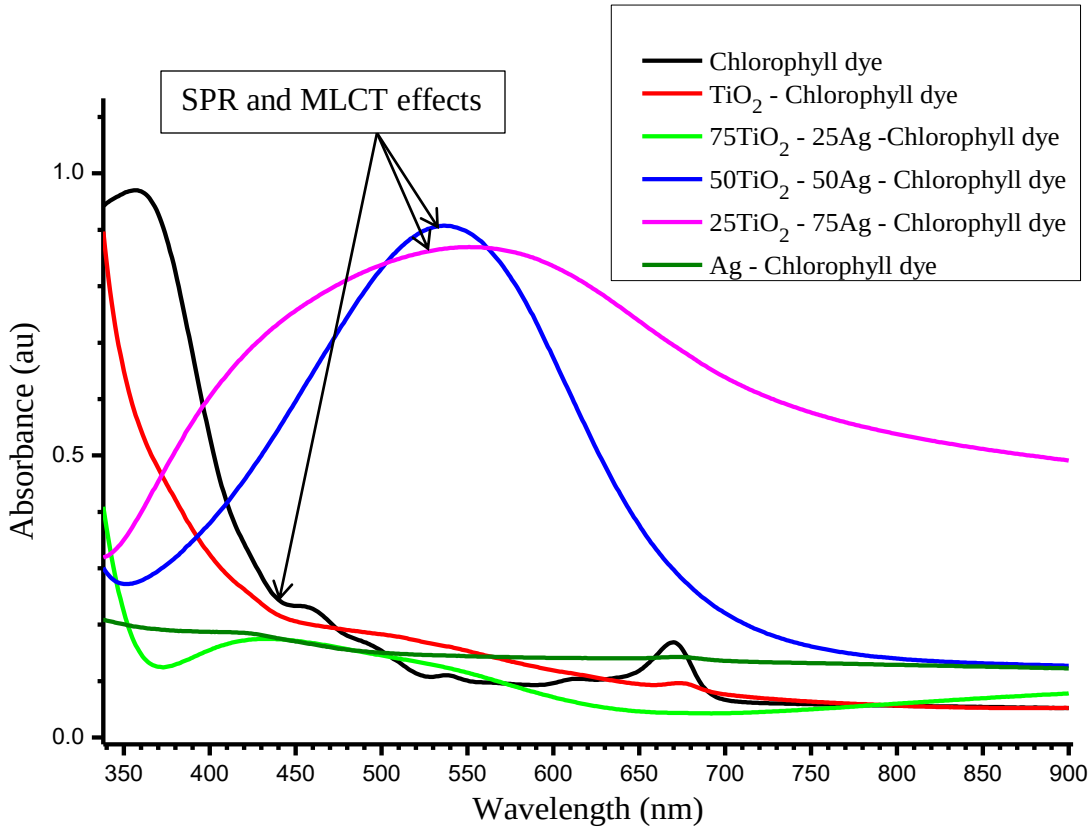

Figure 18 Absorption spectra of the Ag-NP/TiO_2/Chlorophyll dye composite thin films, chlorophyll dye extracted from the Mopane tree leaves.

Both the 100%TiO_2/Chlorophyll dye and 100%Ag-NP/Chlorophyll dye thin film showed absorbance peaks that were enhanced towards the longer wavelength of 500 nm. The thin films consisting of the 25%Ag-NP/75%TiO_2/Chlorophyll dye composition showed a broad absorbance peak extended towards longer wavelengths (400 nm to 550 nm), with peak maximum at ~460 nm. The 50%Ag-NP/50%TiO_2/Chlorophyll dye thin film showed a strong distinctive absorption peak in the range of 400 nm to 650 nm, with absorbance peak maximum at ~540 nm, comparing this thin film to that of 50%Ag-NP/50%TiO_2 thin film in Figure 16, there is definitely an enhancement.

The thin film of the composition 75%Ag-NP/25%TiO_2/Chlorophyll dye showed a strong broader absorbance peak that cover the part of the UV-region, visible region and extend to the near infrared of the spectrum. This absorbance peak lays in the wavelength range 350 nm to 760 nm, with absorbance peak maxims at ~570 nm. These remarkable results could be explained by the unique properties, the SPR and MLCT; and the coupling between the dye and plasmon resonance, leading to the enhancement of charge separation by improving the absorption of the dye [77]. The photo response and photocatalytic activities of TiO_2 are further increased throughout the visible region.

b) Chlorophyll dye extracted from Makalani leaves

Figure 19 represent the UV-VIS absorption spectra of Ag-NP/TiO_2/Chlorophyll dye composite thin films. The dye used was extracted from Makalani tree leaves, using methanol as a solvent. The 100%TiO_2/Chlorophyll dye thin film showed an absorbance peak in the wavelength range of 440 nm to 600 nm, with the absorbance peak maxims at ~520 nm, this response of the peak at about 520 nm indicate metal-to-ligand charge transfer [77]. The 100%Ag-NP/Chlorophyll dye thin film, showed a shift in absorbance peaks, from 410 nm of the 100%Ag-NPs in figure 16 to 520 nm, which can be explained by the coupling between the dye and plasmon resonance [77].

The 25%Ag-NP/75%TiO_2/Chlorophyll dye, 50%Ag-NP/50%TiO_2/Chlorophyll dye and 75%Ag-Np/25%TiO_2/Chlorophyll dye thin films presented wide stronger broader absorption peaks with the wavelength range of 370 nm to 650 nm, 370 nm to 690 nm, and 370 nm to 710 nm respectively. This enhanced absorption and broadened spectrum absorption range of the thin films could be mainly caused by the SPR of Ag-NPs, which

interacted with the dye, enhancing both the dye and TiO_2 absorption that resulted in more charge carrier generation [11, 77].

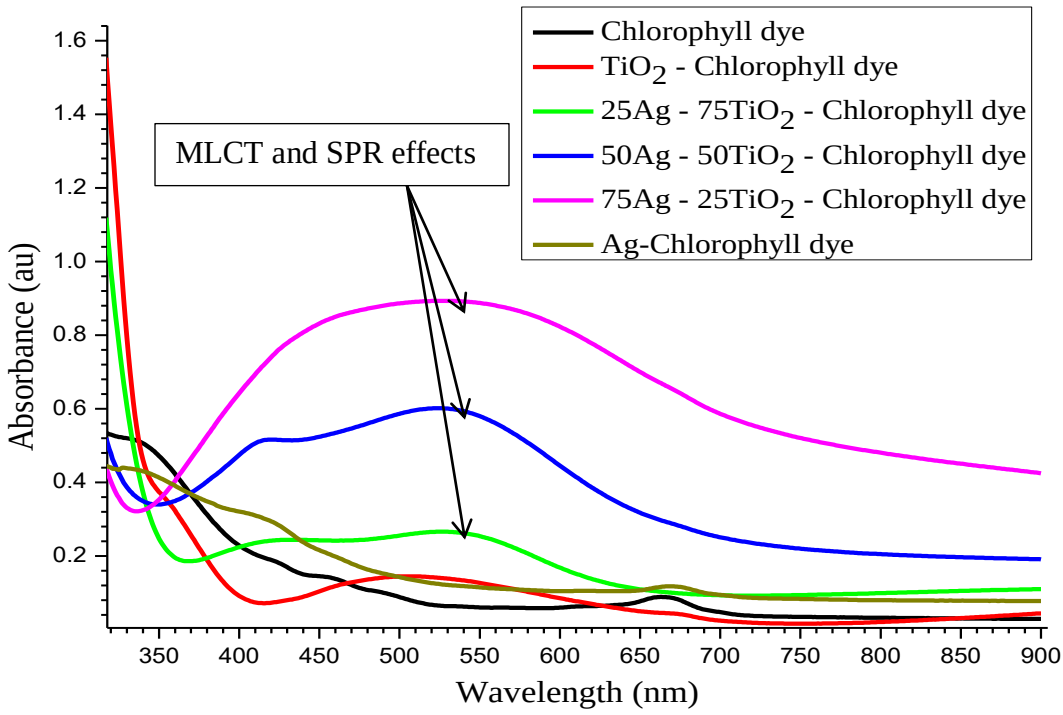

Figure 19 Absorption spectra of Ag-NP/TiO_2/Chlorophyll dye composite thin films, chlorophyll dye extracted from Makalani tree leaves.

4.5 Calculation of the optical band gap

4.5.1 Optical band gap of Ag-NP/TiO_2 composite thin films

By studying the absorption band edge of the spectra presented in figure 20, the TiO_2 thin film showed a low-intensity absorption band in the vis-region; however, its absorption intensity increased steeply (band edge) at shorter wavelengths. In contrast, the Ag NP film showed a strong and broad absorption band at around 410 nm; however its

absorption band edge shifted to shorter wavelengths in the UV region upon increasing the Ag content in TiO_2.

This demonstrated that the Ag particles in the TiO_2 matrix did not narrow the band gap of TiO_2. When Ag NP film is irradiated with vis-light, a large oscillating electric field is observed around the metal particles [25]. The absorption band in the visible region corresponds to the SPR characteristic of Ag NPs. The band gaps remains as that of pure TiO_2 as shown in figure 20, calculated using Tacs expression using a direct band gap value. The band gap was found to be 3.50 as reported by Nagai et al [30] and Daniel et al [25].

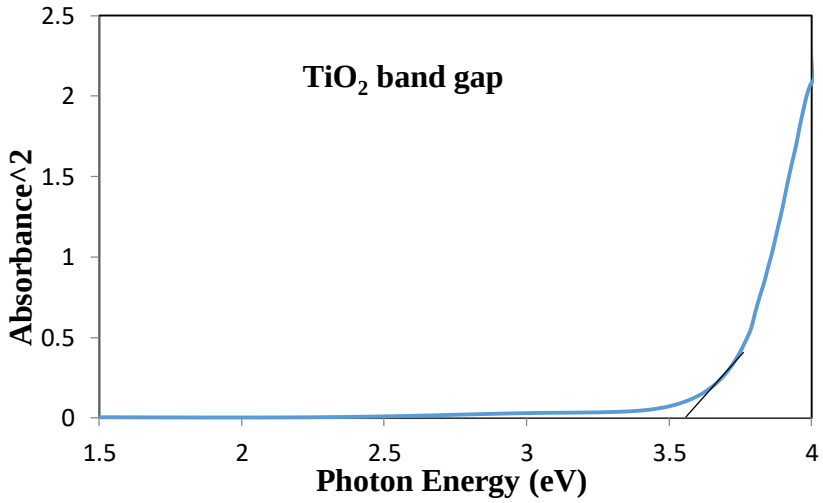

Figure 20 Optical band gap values for TiO_2 thin films. The extrapolation of the straight line of $\alpha = 0$ give the direct band gap of 3.50 eV.

4.5.2 Optical band gap of Ag-NP/TiO_2/Chlorophyll dye composite thin films

Table 3 presents the band gaps in electron volts (eV) extrapolated from the straight line of $\alpha = 0$. The wide band gap of TiO_2 is narrowed when the dye was added. It even decreased further with an increase of Ag-nanoparticles in TiO_2.

Table 3 Shows a summarized optical band gap of the fabricated thin films.

Notation	Band gap (eV)		
	Thin films without chlorophyll dye	Thin films with Chlorophyll dye	
		From Mopane leaves	From Makalani leaves
TiO_2	3.50	3.34	3.2
25%Ag-NP/75%TiO_2	3.50	1.9	1.8
50%Ag-NP/50%TiO_2	3.50	1.7	1.7
75%Ag-NP/25%TiO_2	3.50	1.4	1.4
Ag-NP	-	-	-
Chlorophyll dye	-	1.8	1.8

The band gap of the fabricated thin films was in the range of 1.4 and 3.50 eV, with 75%Ag-Np/TiO_2/Chlorophyll dye thin film with lowest band gap of 1.4 eV and highest band gap of 3.5 eV obtained from the TiO_2 thin film, this is the same as the one reported for TiO_2 thin films fabricated by Molecular precursor method [30, 43]. The band gap of the chlorophyll dye was 1.8 eV, which is the same as those reported in literature [49]. The non-metal substitutional doping of TiO_2 was early claimed as a method for

narrowing the band gap by exclusively changing the valence band structure. Today it is well known that the introduction of non-metal such as N, C and S [2, 20, 25] impurity in TiO_2 do shift the energy levels above the parent TiO_2 valence enabling the thin film to be responsive to Vis light [4]. By doping TiO_2 with silver nanoparticles and chlorophyll dye (made up of mainly C and N), the TiO_2 band gap actually got reduced, hence improving and shifting the threshold of the photo-response of TiO_2 into the visible region. This is due to the presence of the dye, where by the TiO_2 – Dye charge transfer transition, through which the photoelectric charge is injected into the TiO_2 [11, 10] as illustrated in figure 21.

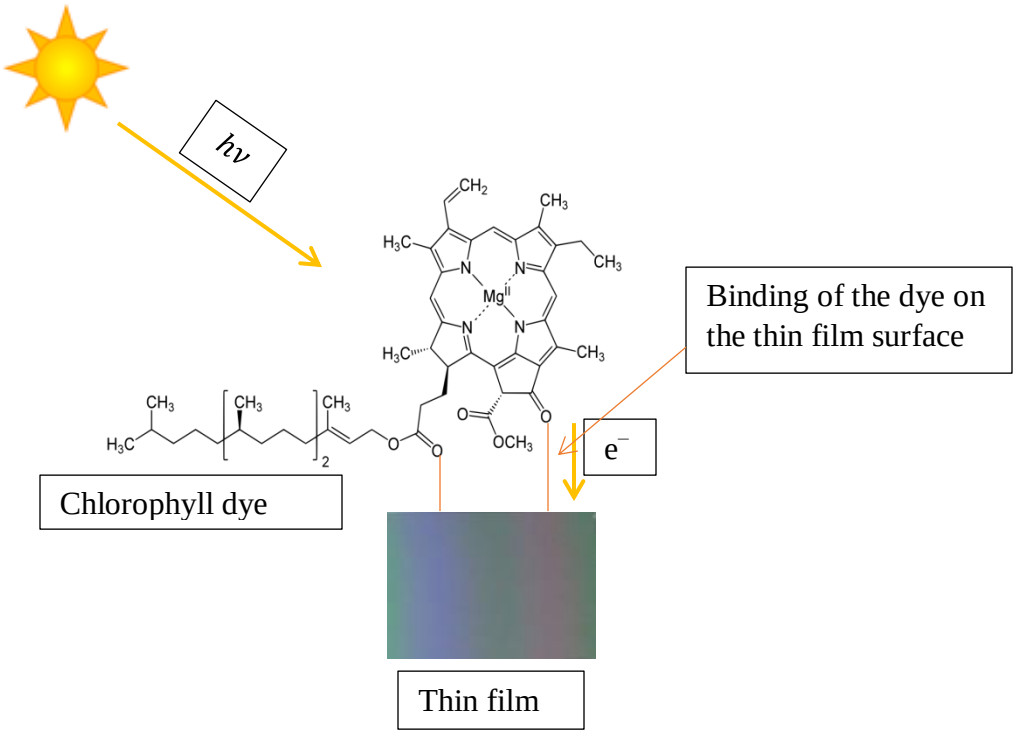

Figure 21: Illustrating the absorption of photon for Ag-NP/TiO_2/Chlorophyll dye thin film.

Currently there appears to be some agreement on the mechanism of nitrogen from Chlorophyll doped visible light absorption explained by Nagai et al., [30] and seconded

by Daniel [31]. All the three articles explained that TiO_2 oxygen lattice sites substituted by nitrogen atoms form an occupied mid gap (N−2p) level above the (O−2p) valence band. Irradiation with UV light (hv ≤380 nm) excites electrons in both the valence band and the narrow (N−2p) band, but irradiating with visible light (hv >380) nm only excites electrons in the narrow (N−2p) band. Based on band structure analysis, a plasmonic-band gap narrowing mechanism is proposed in figure 21; namely, two-step visible-light absorption is caused by the localized surface plasmon resonance of metallic Ag nanoparticles and the band gap photoexcitation of TiO_2. The present results thus suggests that metallic Ag nanoparticles and the dye can act as an effective active component for the construction of a plasmonic-band gap narrowing visible-light mechanism, illustrated in figure 22 below.

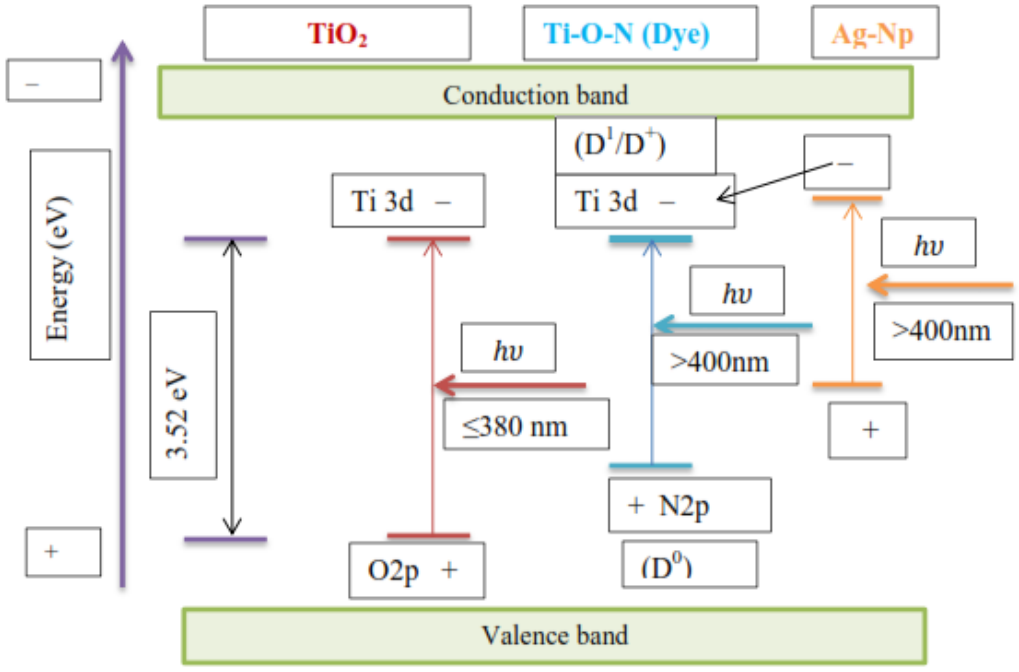

Figure 22: Schematic diagram of the absorption of photon Ag-NP/TiO_2/Chlorophyll dye thin film.

Figure 21 and Figure 22 demonstrate an engineering mechanism explaining the observation happening between the Chlorophyll dye and metal semiconductor during the action of visible light. D^0, D^1 and D^+ are the sensitizer in the ground, excited, and one-electron oxidized states respectively. This titled as a plasmonic-band gap narrowing visible-light mechanism.

CHAPTER 5: CONCLUSIONS AND RECOMMENDATIONS

5.1 Conclusions

In this study thin films were fabricated using the molecular precursor method (MPM) to investigate the optical properties. The chlorophyll dye was successfully extracted from the Mopane and Makalani leaves; and the composite thin films (the Ag-NP/TiO_2composite thin films and the Ag-NP/TiO_2/Chlorophyll dye sensitizers' composite thin films) were successfully fabricated. The absorption properties of the fabricated thin films were successfully characterized using the UV-vis Spectrophotometer.

Based on the results that were obtained, TiO_2 can actually be enhanced by Ag-NPs and the Chlorophyll dye, the absorption of TiO_2 was extended into the ultraviolet to the near-field amplitude at well-defined wavelengths in the visible region, in the wavelength range of 380 nm to 730 nm. These remarkable increments can be explained by the metal-to-ligand charge transfer, through which the photoelectric charge is injected into the TiO_2 and the coupling between the dye and plasmon resonance, leading to the enhancement of charge separation by improving the absorption of the dye. The band gap of undoped TiO_2 was reduced from 3.50 eV to 1.4 eV for TiO_2 when doped with Ag-NPs and Chlorophyll dye. These results can be used in fabrication of photovoltaic devices and water heating systems.

It was learned that when the amount of Ag nanoparticles were increased in the TiO_2 matrix, it resulted in the exhibition of plasmon peak at 410 nm and increased the absorption of the composite thin films, due to the band gap narrowing, hence improving the photo response and photocatalytic properties of TiO_2. When the Chlorophyll dye was adsorbed onto the Ag-NP/TiO_2 composite thin films, it improved and shifted the threshold of the photo-response of Ag-NP/TiO_2 composite thin films into the visible region.

5.2 Recommendations

Further studies that can be done on this research are: to investigate the photocurrent density of the doped TiO_2 and to construct a dye sensitizer solar cells (DSSC) using the obtained thin films; to extract the dye from fresh leaves of plants, controlling the temperature and investigate the stability of the dye extracted.

6. REFERENCES

[1] T.-H. Xu, C.-L. Song, Y. Liu, G.-R. Han. Band structures of TiO_2 doped with N, C and B. *J. Zhejiang U. Sc. B*., 2006; 7: 299-303.

[2] Karabay I, Yüksel SA, Ongül F, Öztürk S, Ash M. Structural and Optical Characterization of TiO_2 Thin Films Prepared by Sol-Gel Process. *Acta Physica Polonica-Series A General Physics*. 2012; 121 (1): 265

[3] Essalhi Z, Hartiti B, Lfakir A, Siadat M, Thevenin P. Optical properties of TiO_2 Thin films prepared by Sol Gel method. *J. Mater. Environ. Sci*.. 2016; 7 (4): 1328-1333.

[4] Likius DS. Electrical conductivities, plasmonic properties and vis-responsive activities of Ag-Nanoparticles/Titania composite thin films fabricated using molecular precursor method (MPM) (Doctoral dissertation), Kogakuin University (Tokyo, Japan).

[5] Criado J, Real C. Mechanism of the inhibiting effect of phosphate on the anatase-rutile transformation induced by thermal and mechanical treatment of TiO_2. *Journal of the Chemical Society, Faraday Transactions 1: Physical Chemistry in Condensed Phases*. 1983; 79 (12): 2765-2771.

[6] Ermolli I, Matthes K, Dudok de Wit T, Krivova NA, Tourpali K, Weber M, Unruh YC, Gray L, Langematz U, Pilewskie P, Rozanov E. Recent variability of the solar spectral irradiance and its impact on climate modelling. *Atmospheric Chemistry and Physics*. 2013; 13 (8): 3945-3977.

[7] Zhang J, Zou H, Qing Q, Yang Y, Li Q, Liu Z, Guo X, Du Z. Effect of chemical oxidation on the structure of single-walled carbon nanotubes. *The Journal of Physical Chemistry B*. 2003; 107 (16): 3712-3718.

[8] Rehman S, Ullah R, Butt AM, Gohar ND. Strategies of making TiO_2 and ZnO visible light active. *Journal of hazardous materials*. 2009; 170 (2): 560-569.

[9] Nasr-Esfahani M, Habibi MH. Silver doped TiO_2 nanostructure composite photocatalyst Film Synthesized by sol-gel spin and dip coating technique on glass. *International Journal of Photoenergy*. 2008.

[10] Veikko U, Zhang X, Peng T, Cai P, Cheng G. The synthesis and characterization of dinuclear ruthenium sensitizers and their applications in photocatalytic hydrogen production. *Spectrochimica Acta Part A: Molecular and Biomolecular Spectroscopy*. 2013; 105: 539-544.

[11] Ryan M. PGM HIGHLIGHTS: Progress in Ruthenium Complexes for Dye Sensitised Solar Cells. *Platinum Metals Review*. 2009; 53 (4): 216-218.

[12] Richhariya G, Kumar A, Tekasakul P, Gupta B. Natural dyes for dye sensitized solar cell: A review. *Renewable and Sustainable Energy Reviews*. 2017; 69: 705-718.

[13] Pujiarti H, Arsyad WS, Wulandari P, Hidayat R. The effect of ionic liquid electrolyte concentrations in dye sensitized solar cell using gel electrolyte. *InAIP Conference Proceedings* 2014: 39-42.

[14] Syafinar R, Gomesh N, Irwanto M, Fareq M, Irwan YM. "Chlorophyll pigments as nature based dye for dye-sensitized solar cell (DSSC)," *Energy Procedia*. 896 – 902.

[15] Mozaffari SA, Saeidi M, Rahmanian R. Photoelectric characterization of fabricated dye-sensitized solar cell using dye extracted from red Siahkooti fruit as natural sensitizer. *Spectrochim Acta A: Mol Biomol Spectrosc*. 142 (2015); 226-231.

[16] Bhogaita M, Shukla AD, Nalini RP. Recent advances in hybrid solar cells based on natural dye extracts from Indian plant pigment as sensitizers. *Solar Energy*. 2016; 137: 212-224.

[17] Behnajady MA, Modirshahla N, Shokri M, Rad B. Enhancement of photocatalytic activity of TiO_2 nanoparticles by silver doping: photodeposition versus liquid impregnation methods. *Global NEST Journal*. 2008; 10 (1): 1-7.

[18] Platzer MD. US solar photovoltaic manufacturing: Industry trends, global competition federal support. Washington, DC: *Congressional Research service*. 2012. 3; 6.

[19] Kaminski-Cachopo A. Solar cells for energy harvesting. Web blog. Available from: https://www.nereid-h2020.eu/system/files/files/workshops/DWS/slides/DWS_WP42-2016-1019-02Kaminski_NEREID_public.pdf [Accessed 02 September 2018].

[20] Irie H, Miura S, Kamiya K, Hashimoto K. Efficient visible light-sensitive photocatalysts: grafting Cu (II) ions onto TiO_2 and WO_3 photocatalysts. *Chemical Physics Letters*. 2008; 457 (1-3): 202-205.

[21] Litter MI. Heterogeneous photocatalysis: transition metal ions in photocatalytic systems. *Applied Catalysis B: Environmental*. 1999; 23 (2-3): 89-114.

[22] Georgieva J. TiO_2/WO_3 photoanodes with enhanced photocatalytic activity for air treatment in a polymer electrolyte cell. *Journal of Solid State Electrochemistry*. 2012; 16 (3): 1111-1119.

[23] Bhawana P, Fulekar MH. Nanotechnology: remediation technologies to clean up the environmental pollutants. *Res. J. chem. sci*. 2012; 2 (2): 90-96.

[24] Anandhan S, Bandyopadhyay S. Polymer nanocomposites: from synthesis to applications. *InNanocomposites and polymers with analytical methods*. 2011.

[25] Daniel LS, Nagai H, Yoshida N, Sato M. Photocatalytic activity of vis-responsive Ag-nanoparticles/TiO_2 composite thin films fabricated by molecular precursor method (MPM).. 2013; 3 (3): 625-645.

[26] Li H, Zhao G, Song B, Han G. Effect of incorporation of silver on the electrical properties of sol-gel-derived titania film. *Journal of Cluster Science*. 2008; 19 (4): 667-673.

[27] Cattin L, Morsli M, Dahou F, Abe SY, Khelil A, Bernède JC. Investigation of low resistance transparent MoO_3/Ag/MoO_3 multilayer and application as anode in organic solar cells. *Thin Solid Films*. 2010; 518 (16): 4560-4563.

[28] Kumpika T, Thongsuwan W, Singjai P. Optical and electrical properties of ZnO nanoparticle thin films deposited on quartz by sparking process. *Thin Solid Films*. 2008; 516 (16): 5640-5644.

[29] Zhao G, Kozuka H, Yoko T. Sol—gel preparation and photoelectrochemical properties of TiO_2 films containing Au and Ag metal particles. *Thin solid films*. 1996; 277 (1-2): 147-154.

[30] Nagai H, Mochizuki C, Hara H, Takano I, Sato M. Enhanced UV-sensitivity of vis-responsive anatase thin films fabricated by using precursor solutions involving Ti complexes. *Solar Energy Materials and Solar Cells*. 2008; 92 (9): 1136-1144.

[31] Likius DS, Nagai H, Aoyama S, Mochizuki C, Hara H, Baba N, Sato M. Percolation threshold for electrical resistivity of Ag-nanoparticle/titania composite thin films fabricated using molecular precursor method. *Journal of Materials Science*. 2012; 47 (8): 3890-3899.

[32] Balamurugan M, Kandasamy N, Saravanan S, Ohtani N. Synthesis of uniform and high-density silver nanoparticles by using Peltophorum pterocarpum plant extract. *Japanese Journal of Applied Physics.* 2014; 53 (5S1): 05FB19.

[33] Marciello M, Luengo Y, Morales MP. Iron Oxide Nanoparticles for Cancer Diagnosis and Therapy. *Nanoarchitectonics for Smart Delivery and Drug Targeting*. 2016: 667-693.

[34] Wang Z, Helmersson U, Käll PO. Optical properties of anatase TiO_2 thin films prepared by aqueous sol–gel process at low temperature. *Thin Solid Films*. 2002; 405 (1-2): 50-54.

[35] Nagai H, Sato M. Heat treatment in molecular precursor method for fabricating metal oxide thin films. *InHeat Treatment-Conventional and Novel Applications* 2012. InTech.

[36] Ayser JI, Bushra KH, Khudayer IH. Effect Ambient Oxidation on Structural and Optical Properties of Copper Oxide Thin Films. *International journal of Innovative Research in Science, Engineering and Technology*.

[37] Izaki M, Shinagawa T, Mizuno KT, Ida Y, Inaba M, Tasaka A. Electrochemically constructed p-Cu_2O/n-ZnO heterojunction diode for photovoltaic device. *Journal of Physics D: Applied Physics.* 2007; 40 (11): 3326.

[38] Andronescu E, Grumezescu AM, Gusa MI, Holban AM, Ilie FC, Irimia A, Nicoara IF, Tone M. Nano-hydroxyapatite: novel approaches in biomedical applications. *Nanobiomaterials in Hard Tissue Engineering.* 2016: 189-213.

[39] Yuhas BD, Yang P. Nanowire-based all-oxide solar cells. *Journal of the American Chemical Society.* 2009. 131 (10): 3756-3761.

[40] Sakka S. Handbook of Sol-Gel Science and Technology. Handbook of Advanced Ceramics. 2016: 883-910.

[41] Guo K, Li M, Fang X, Liu X, Sebo B, Zhu Y, Hu Z, Zhao X. Preparation and enhanced properties of dye-sensitized solar cells by surface plasmon resonance of Ag

nanoparticles in nanocomposite photoanode. *Journal of Power Sources*. 2013; 230: 155-160.

[42] Daniel LS, Nagai H, Sato M. Absorption spectra and photocurrent densities of Ag nanoparticle/TiO_2 composite thin films with various amounts of Ag. *Journal of materials science.* 2013 Oct 1;48(20):7162-7170.

[43] Daniel LS, Nagai H, Sato M. Photoelectrochemical property and the mechanism of plasmonic Ag-NP/TiO_2 composite thin films with high silver content fabricated using molecular precursor method. *Journal of Mater Sci*. 2013; 48:7162-7170.

[44] Vaghasiya JV, Sonigara KK, Fadadu KB, Soni SS. Hybrid AgNP–TiO_2 thin film based photoanode for dye sensitized solar cell. *Perspectives in Science*. 2016; 8: 46-49.

[45] Velmurugan R, Krishnakumar B, Swaminathan M. Synthesis of Pd co-doped nano-TiO_2–SO42–and its synergetic effect on the solar photodegradation of Reactive Red 120 dye. *Materials Science in Semiconductor Processing*. 2014; 25: 163-172.

[46] Zhang W, Dehghani-Sanij AA, Blackburn RS. Carbon based conductive polymer composites. *Journal of materials science*. 2007; 42 (10): 3408-3418.

[47] Elechiguerra JL, Burt JL, Morones JR, Camacho-Bragado A, Gao X, Lara HH, Yacaman MJ. Interaction of silver nanoparticles with HIV-1. *Journal of nanobiotechnology*. 2005; (1): 6.

[48] Lin YC. Applying Ag–TiO 2/functional filter for abating odor exhausted from semiconductor and opti-electronic industries. *Clean Technologies and Environmental Policy*. 2013; 15 (2): 359-366.

[49] Syafinar R, Gomesh N, Irwanto M, Fareq M, Irwan YM. Chlorophyll pigments as nature based dye for dye-sensitized solar cell (DSSC). *Energy Procedia.* 2015; 79: 896-902.

[50] Baysal A, Aydemir M, Durap F, Özkar S, Yıldırım LT, Ocak YS. A ruthenium (II) bipyridine complex containing a 4, 5-diazafluorene moiety: Synthesis, characterization and its applications in transfer hydrogenation of ketones and dye sensitized solar cells. *Polyhedron*. 2015; 89: 55-61.

[51] Jin Z, Masuda H, Yamanaka N, Minami M, Nakamura T, Nishikitani Y. Efficient electron transfer ruthenium sensitizers for dye-sensitized solar cells. *The Journal of Physical Chemistry C*. 2009; 113 (6): 2618-2623.

[52] Bae H, Lee C, Baek J, Yang H.'Novel Ru-Type Sensitizers and Method of Preparing the Same'. *World Appl*. 2009; 082,163.

[53] Obotowo IN, Obot IB, Ekpe UJ. Organic sensitizers for dye-sensitized solar cell (DSSC): Properties from computation, progress and future perspectives. *Journal of Molecular Structure*. 2016; 1122: 80-87.

[54] Lee CP, Li CT, Ho KC. Use of organic materials in dye-sensitized solar cells. *Materials Today*. 2017.

[55] Selopal GS, Wu HP, Lu J, Chang YC, Wang M, Vomiero A, Concina I, Diau EW. Metalfree organic dyes for TiO2 and ZnO dye-sensitized solar cells. *Scientific reports*. 2016; 6.

[56] Calogero G, Di Marco G, Caramori S, Cazzanti S, Argazzi R, Bignozzi CA. Natural dye senstizers for photoelectrochemical cells. *Energy & Environmental Science*. 2009; 2(11): 1162-1172.

[57] Grätzel M, Innovation, 2007, 7, (3), cover story.

[58] Michaelis L, Schubert MP, Smythe CV. "Potentiometric Study of the Flavins". *J. Biol. Chem*. 1936: 116 (2): 587–607.

[59] Stafford HA (1994). "Anthocyanins and betalains: evolution of the mutually exclusive pathways". *Plant Science*. 1994: 101 (2): 91–98.

[60] Al-Alwani MA, Ludin NA, Mohamad AB, Kadhum AA, Sopian K. Extraction, preparation and application of pigments from Cordyline fruticosa and Hylocereus polyrhizus as sensitizers for dye-sensitized solar cells. *Spectrochimica Acta Part A: Molecular and Biomolecular Spectroscopy*. 2017; 179: 23-31.

[61] Harris DC. Quantitative chemical analysis. 8th ed. United States of America. Clancy Marshall; 2010.

[62] Kumar S. Spectroscopy of Organic Compounds. Web blog. Available from: http://www.uobabylon.edu.iq/eprints/publication_11_8282_250.pdf [Accessed 2nd October 2018].

[63] James WR, Eileen MSF, George MF. Undergraduate instrumental analysis. 7th ed. 2014.

[64] Weckhysen B M. Ultraviolet – Visible Spectroscopy. *American Scientific Publishers*. 2004; 255-270.

[65] Ewing GW. Analytical instrumentation handbook. 2nd ed. United states of America. Marcel Dekker, INC; 1997.

[66] Pg instruments. Uv-visible spectrophotometer. Web blog. Available from: http://www.an-ka.com/uploads/PG%20UV-VIS%20Spectrophotometer%20Print%20Catalogue.pdf [Accessed 4th October 2018].

[67] Introduction to FTIR spectroscopy. Web blog. Available from: https://www.thermofisher.com/na/en/home/industrial/spectroscopy-elemental-isotope-analysis/spectroscopy-elemental-isotope-analysis-learning-center/molecular-

spectroscopy-information/ftir-information/ftir-basics.html [Accessed 14th September 2018].

[68] How an FTIR Spectrometer Operates. Web blog. Available from: https://chem.libretexts.org/Textbook_Maps/Physical_and_Theoretical_Chemistry_Textbook_Maps/Supplemental_Modules_(Physical_and_Theoretical_Chemistry)/Spectroscopy/Vibrational_Spectroscopy/Infrared_Spectroscopy/How_an_FTIR_Spectrometer_Operates [Accessed 15th September 2018].

[69] Band gap. Web blog. [Online]. Available from: https://energyeducation.ca/encyclopedia/Band_gap [Accessed 14th September 2018].

[70] PV Education. Band Gap. Web blog. [Online]. Available from: http://www.pveducation.org/pvcdrom/pn-junction/band-gap [Accessed 15th September 2018].

[71] Ray SC. Preparation of copper oxide thin film by the sol–gel-like dip technique and study of their structural and optical properties. *Solar energy materials and solar cells*. 2001; 68 (3): 307-312.

[72] Zhou H, Wu L, Gao Y, Ma T. Dye-sensitized solar cells using 20 natural dyes as sensitizers. *Journal of Photochemistry and Photobiology A: Chemistry*. 2011; 219 (2-3): 188-194.

[73] Saravanan S, Kato R, Balamurugan M, Kaushik S, Soga T. Efficiency improvement in dye sensitized solar cells by the plasmonic effect of green synthesized silver nanoparticles. *Journal of Science: Advanced Materials and Devices*. 2017; (4): 418-424.

[74] Ramamoorthy R, Radha N, Maheswari G, Anandan S, Manoharan S, Williams RV. Betalain and anthocyanin dye-sensitized solar cells. *Journal of Applied Electrochemistry*. 2016; 46 (9): 929-941.

[75] Chang H, Lo YJ. Pomegranate leaves and mulberry fruit as natural sensitizers for dye-sensitized solar cells. *Solar Energy*. 2010; 84 (10): 1833-1837.

[76] Taya SA, El-Agez TM, El-Ghamri HS, Abdel-Latif MS. Dye-sensitized solar cells using fresh and dried natural dyes. *International Journal of Materials Science and Applications*. 2013; 2 (2): 37-42.

[77] Lin SJ, Lee KC, Wu JL, Wu JY. Plasmon-enhanced photocurrent in dye-sensitized solar cells. *Solar Energy*. 2012; 86 (9):2600-2605.

[78] Matsubara K, Tatsuma T. Morphological changes and multicolor photochromism of Ag nanoparticles deposited on single-crystalline TiO_2 surfaces. *Adv. Mater*. 2007: 19, 2802–2806.

7. APPENDICES

Appendix I: Optical band gap of Ag-NP/TiO_2/Chlorophyll dye composite thin films (the dye extracted from Mopane leaves)

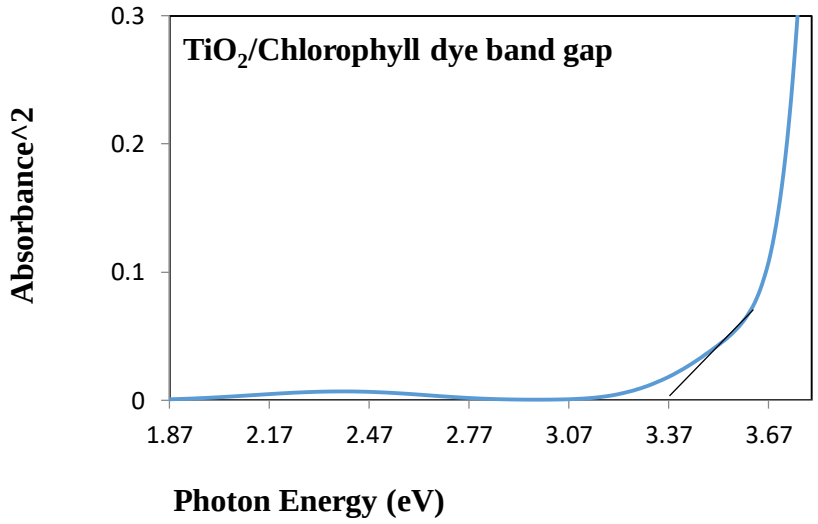

a)

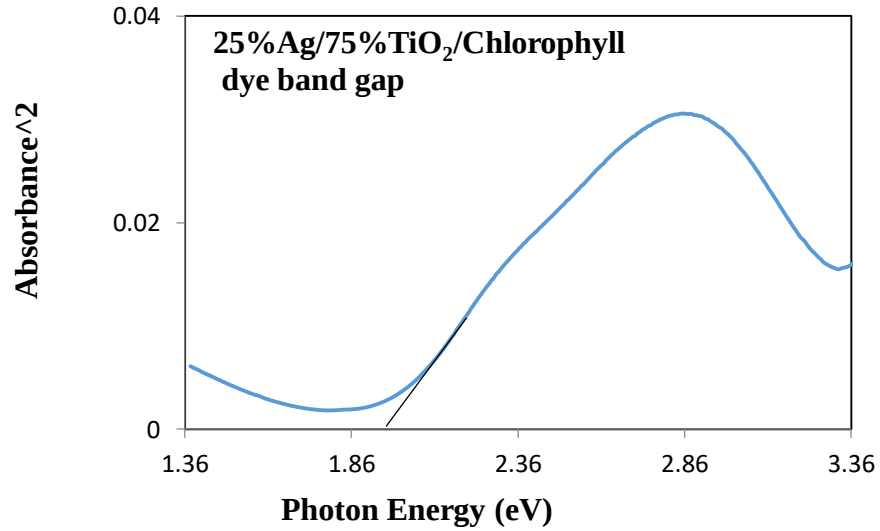

b)

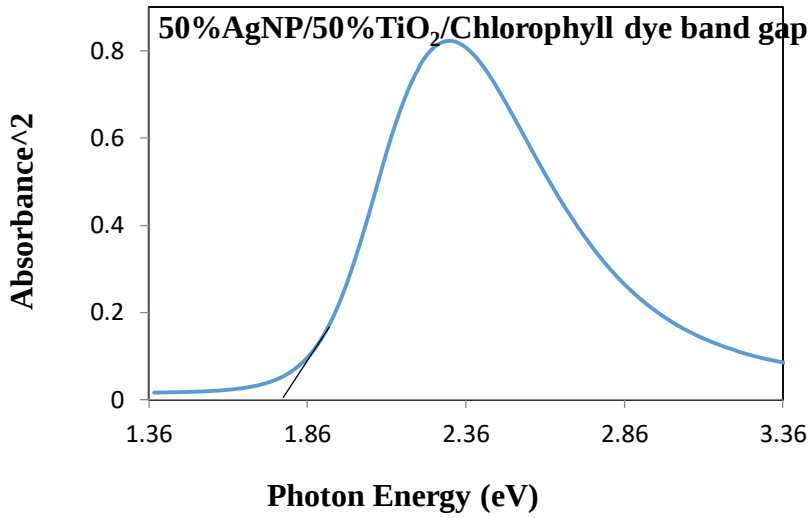
50%AgNP/50%TiO2/Chlorophyll dye band gap
Absorbance^2
0.8
0.6
0.4
0.2
0
1.36
1.86
2.36
2.86
3.36
Photon Energy (eV)

c)

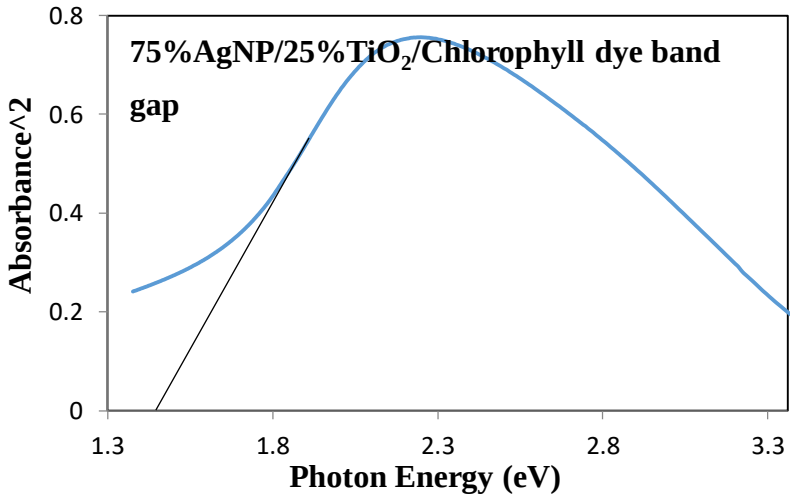
75%AgNP/25%TiO2/Chlorophyll dye band gap
Absorbance^2
0.8
0.6
0.4
0.2
0
1.3
1.8
2.3
2.8
3.3
Photon Energy (eV)

d)

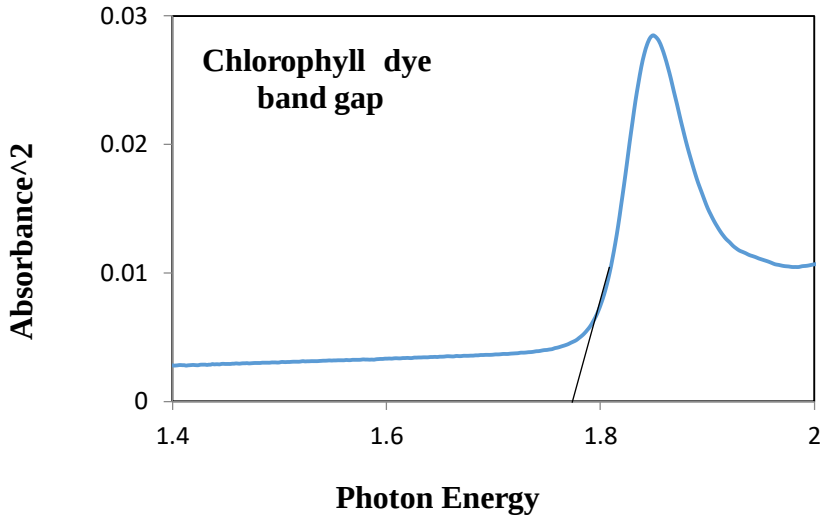

e)

Figure 23 Optical band gap values for Ag-NP/TiO_2/Chlorophyll dye thin films. The extrapolation of the straight line of $\alpha = 0$ gives the direct band gap of 3.3, 1.9, 1.7, 1.4 and 1.78 eV for TiO_2/Chlorophyll dye, 25%Ag-NP/75%TiO_2/Chlorophyll dye, 50%Ag-NP/50%TiO_2/ Chlorophyll dye, 75%Ag-NP/25%TiO_2/Chlorophyll dye and Chlorophyll dye thin film respectively.

Appendix II: Optical band gap of Ag-NP/TiO_2/Chlorophyll dye composite thin films (the dye extracted from Makalani leaves)

The diagrams in figure 23 present the direct band gap (eV) of the Ag-NP/TiO_2/Chlorophyll dye thin films (Chlorophyll dye extracted from the Makalani leaves).

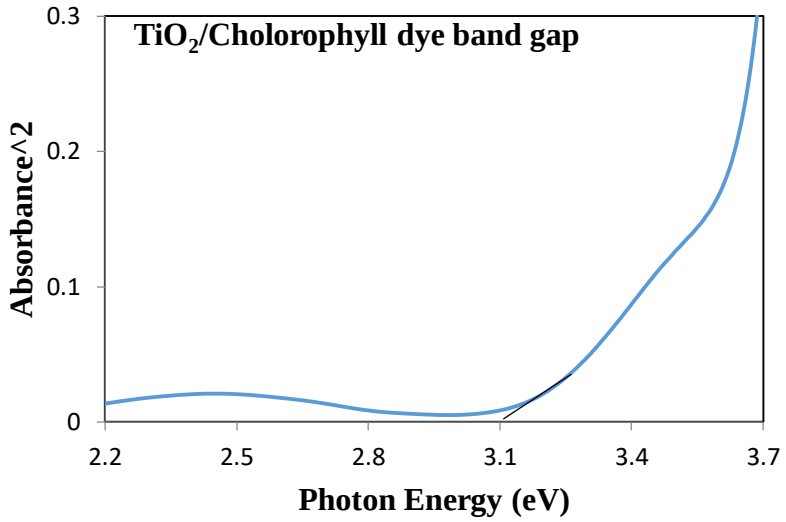
TiO2/Cholorophyll dye band gap
Absorbance^2
0.3
0.2
0.1
0
2.2
2.5
2.8
3.1
3.4
3.7
Photon Energy (eV)

a)

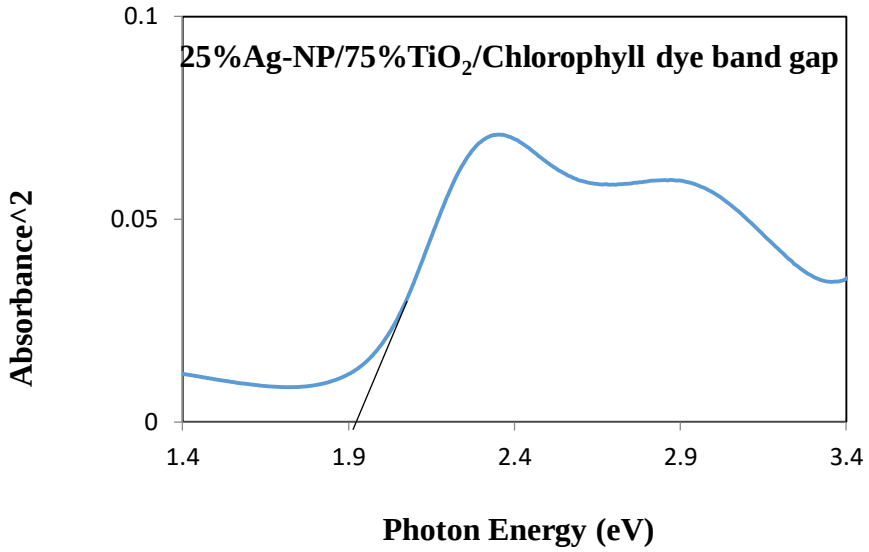
25%Ag-NP/75%TiO2/Chlorophyll dye band gap
Absorbance^2
0.1
0.05
0
1.4
1.9
2.4
2.9
3.4
Photon Energy (eV)

b)

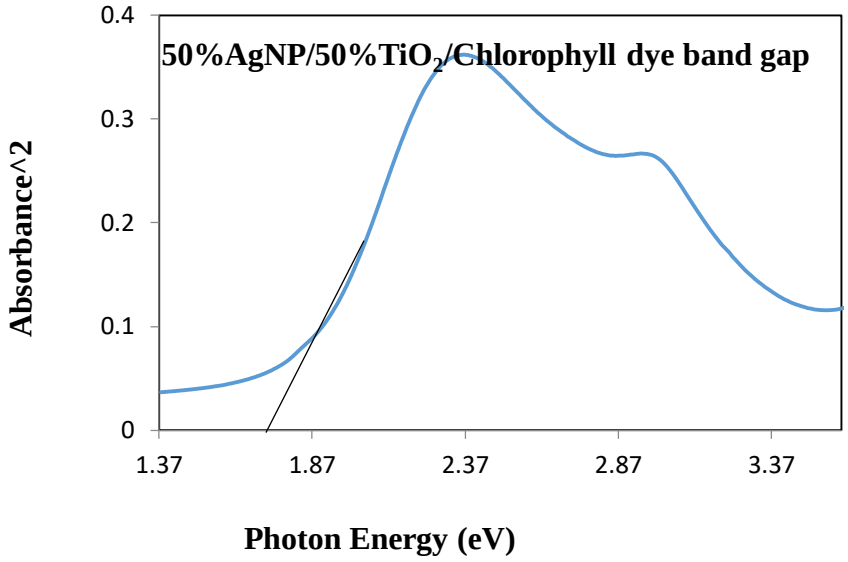
50%AgNP/50%TiO2/Chlorophyll dye band gap
Absorbance^2
0.4
0.3
0.2
0.1
0
1.37
1.87
2.37
2.87
3.37
Photon Energy (eV)

c)

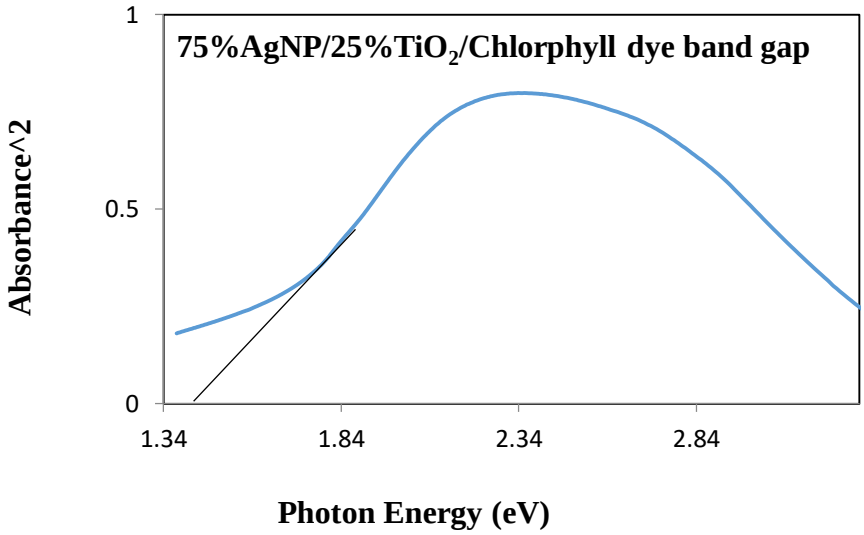
75%AgNP/25%TiO2/Chlorphyll dye band gap
Absorbance^2
1
0.5
0
1.34
1.84
2.34
2.84
Photon Energy (eV)

d)

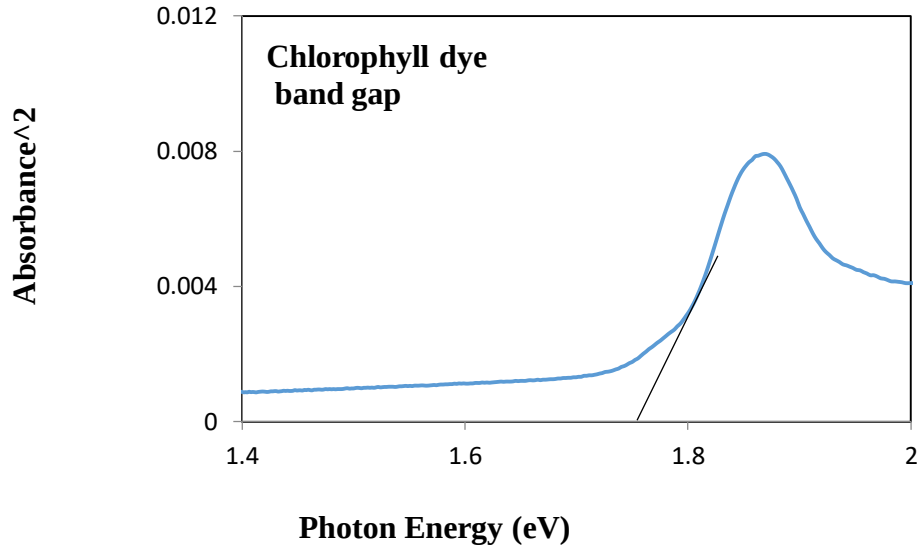

e)

Figure 24 Optical band gap values for Ag-NP/TiO_2/Chlorophyll dye thin films. The extrapolation of the straight line of $\alpha = 0$ gives the direct band gap of 3.2, 1.8, 1.7, 1.4, and 1.76 eV for TiO_2/Chlorophyll dye, 25%Ag-NP/75%TiO_2/Chlorophyll dye, 50%Ag-NP/50%TiO_2/ Chlorophyll dye, 75%Ag-NP/25%TiO_2/Chlorophyll dye, and Chlorophyll dye thin film respectively.